Michał Wasiak

Review of selected papers

Diplomas and scientific degrees

PhD in Physics at the Institute of Physics, Technical University of Lodz. Thesis title: *Optical gain in quantum dot lasers*, November 2004 Supervisor: prof. dr hab. Maciej Bugajski.

MSc in Physics at at the Institute of Physics, Technical University of Lodz. Thesis title: *Optical gain in quantum well lasers*, September 1999. Supervisor: prof. dr hab. Maciej Bugajski.

Career

2005–present Assistant Professor at the Institute of Physics, Lodz University of Technology.

1999–2005 Research Assistant at the Institute of Physics, Technical University of Lodz.

Series of publications: Modelling of physical phenomena in semiconductor lasers

Papers for consideration

[1] **M. Wasiak**. "Quantum-enhanced uniformity of carrier injection into successive quantum wells of multi-quantum-well structures". In: *Physica E: Low-dimensional Systems and Nanostructures* 41.7 (2009), pp. 1253–1257. ISSN: 1386-9477. DOI: 10.1016/j.physe.2009.02.013.

[2] **M. Wasiak**. "Mathematical rigorous approach to simulate an over-threshold VCSEL operation". In: *Physica E: Low-dimensional Systems and Nanostructures* 43.8 (2011), pp. 1439–1444. ISSN: 1386-9477. DOI: 10.1016/j.physe.2011.03.022.

[3] L. Frasunkiewicz, T. Czyszanowski, **M. Wasiak**, M. Dems, R.P. Sarzała, W. Nakwaski, and K. Panajotov. "Optimization of Single-Mode Photonic-Crystal Results in Limited Improvement of Emitted Power and Unexpected Broad Range of Tuning". In: *Journal of Lightwave Technology* 31.9 (May 2013), pp. 1360–1366. ISSN: 0733-8724. DOI: 10.1109/JLT.2013.2247565.
My contribution (20%): Creation of the above-threshold VCSEL model used in the simulations.

[4] **M. Wasiak**, M. Bugajski, and W.Nakwaski. "Envelope function description of quantum cascade laser electronic states". In: *Optica Applicata* 35 (2005).
My contribution (70%): Devising a model for determining states and wave functions in polarised superlattices; performing numerical simulations.

[5] M. Motyka, F. Janiak, J. Misiewicz, **M. Wasiak**, K. Kosiel, and M. Bugajski. "Determination of energy difference and width of minibands in GaAs/AlGaAs superlattices by using Fourier transform photoreflectance and photoluminescence". In: *Opto-Electronics Review* 19 (2011), pp. 151–154.
My contribution (20%): Quantitative theoretical and numerical analysis of intra- and inter-band transitions in superlattices; calculation of the energies and relative intensities of the optical transitions.

[6] Łukasz Piskorski, Michał Wasiak, Robert P. Sarzała, and Włodzimierz Nakwaski. "Tuning effects in optimisation of GaAs-based InGaAs/GaAs quantum-dot VCSELs". In: *Optics Communications* 281.11 (2008), pp. 3163–3170. ISSN: 0030-4018. DOI: 10.1016/j.optcom.2008.02.011.
My contribution (35%): Developing a gain model for quantum dots; analysis of the statistical properties of quantum-dot populations; interpreting of the results of simulations concerning optical gain.

[7] V. Iakovlev, J. Walczak, M. Gębski, A.K. Sokół, **M. Wasiak**, P. Gallo, A. Sirbu, R.P. Sarzała, M. Dems, T. Czyszanowski, and E. Kapon. "Double-diamond high-contrast-gratings vertical external cavity surface emitting laser". In: *Journal of Physics D: Applied Physics* 47.6 (2014), p. 065104.
My contribution (10%): Devising the concept for a thermal model of optically pumped lasers; adjusting the modelling to the fabrication technology used at EPFL.

[8] **M. Wasiak**, R.P. Sarzała, and A. Jasik. "Temperature reduction in vertical-external-cavity surface-emitting-lasers (VECSEL) active region". In: *Transparent Optical Networks, 2009. ICTON '09. 11th International Conference on*. July 2009, pp. 1–3. DOI: 10.1109/ICTON.2009.5185028.
My contribution (60%): Devising the concept for a thermal model of optically pumped lasers; numerical calculations of the thermal properties of different VECSEL structures; analysis of physical phenomena in different types of construction.

[9] **M. Wasiak**, P. Śpiewak, P. Moser, J. Walczak, R.P. Sarzała, T. Czyszanowski, and J.A. Lott. "Numerical model of capacitance in vertical-cavity surface-emitting lasers". In: *Journal of Physics D: Applied Physics* 49.17 (2016), p. 175104.
My contribution (70%): Creation of a model for capacitance and current dynamics in VCSELs; analysis of experimental data.

[10] **M. Wasiak**, P. Śpiewak, P. Moser, and J.A. Lott. *Capacitance and modulation time constant in oxide-confined vertical-cavity surface-emitting lasers with different oxide layers*. Invited talk at Photonics Europe 2016. Brussels, Apr. 2016.
My contribution (70%): Application of a capacitance model and optical models to analysis of modulation parameters in arsenide and nitride VCSELs.

Contents

Diplomas and scientific degrees . . . 1
Career . . . 1
Series of publications: Modelling of physical phenomena in semiconductor lasers . . . 1
Papers for consideration . . . 1
1. Preface . . . 3
2. Tunnelling of carriers in multiple quantum wells [1] . . . 5
3. Above-threshold model [2, 3] . . . 7
4. Quantum cascade lasers and superlattices [4, 5] . . . 9
4.1. Applications of the model . . . 13
5. Quanum dot lasers [6] . . . 14
6. Vertical external cavity surface emitting laser [7, 8] . . . 17
6.1. High contrast grating . . . 20
7. Model of capacitance in semiconductor lasers [9, 10] . . . 22
8. Summary . . . 25
References . . . 28

1. Preface

Physics is a scientific discipline which attempts to describe reality using the language of mathematics. Since this became the dominant paradigm in the field, thanks largely to the celebrated achievements of Isaac Newton, physics has been used mainly to describe idealized objects (material points, spheres, infinite planes etc.), which could, in a certain respect, be thought of as models of the simplest real objects existing in nature. This is due principally to the obvious practical limitations of the application of mathematical methods, but also perhaps to a certain inclination of the human mind towards such idealizations. For example, Johannes Kepler's idea of replacing the complex and not very accurate system of circular epicycles to describe the movements of the planets with elliptical orbits seemed absurd to the brightest minds of the time [11]. This criticism was based on ideology—the circle was believed to be more 'noble' than the ellipse. It was also based on the fact that mathematical formalism could be applied relatively effectively to spheres and points, but becomes cumbersome when applied to real objects. The idealizing tendency is manifested today by the fact that physics can say much about things no one has seen (such as quarks, or the Big Bang), but when it comes to everyday objects and phenomena, such as the behavior of living creatures or the weather, its powers of prediction seem weak by comparison.

Although it seems that certain physical theories (for example Maxwell's equations or, more generally, quantum electrodynamics [12]) are absolutely accurate within the limits of their application, for practical reasons we can apply them only to the simplest objects. Thanks to our knowledge of physics, we can create devices which do not exist in nature, but which we can build from circles, spheres, cubes, cylinders, rods, and so on. Semiconductor devices made from rectangular parallelepipeds, provide a good example. Irregularities which occur during the fabrication process usually adversely affect the devices' performance, so monocrystalline solids are used and efforts are made to avoid any such

dislocations. Although this might seem perfectly reasonable, it is not necessarily the best approach. In the natural world regular objects are rare, but organs, tissues, even individual cells are such effective mechanisms that often we cannot fabricate anything comparable—in many cases, even when we consider them in the simplest form, as chemical reactors.

An additional, mathematical rather than physical, obstacle is the complexity of the calculations required by the models. These are mostly numerical calculations, which generate specific kinds of problem, such as convergence and numerical errors. This can cause very serious errors which are, however, difficult to detect. Unfortunately, physicists who use numerical methods often lack the knowledge necessary to avoid such problems, while specialized mathematicians rarely focus on problems in physics.

The papers presented here concern a class of nanotechnological devices, namely, contemporary semiconductor lasers. These are simple enough (in the sense presented above) that we can model them, predict and explain their properties, often even quantitatively (assuming a certain tolerance). Although such devices are relatively simple, they require a self-consistent combination of models related to very different physical phenomena:

1. electric current and diffusion of the carriers
2. heat generation and flow
3. electromagnetic wave propagation
4. quantum effects in quantum wells, quantum dots, superlattices, etc.

Theories relating to the first two phenomena were developed in the 19th century and are still in use (except in some areas of semiconductor laser research, where quantum effects can lessen their validity). Maxwell's equations, which describe electromagnetic waves, were also formulated in the 19th century, but their status is rather different. Their validity and accuracy has not so far been falsified in any experiments, and they serve as the basis of, for instance, the theory of relativity. In contrast, electrons in solid states and their interactions with electromagnetic fields can only be described using the theory of quantum mechanics—which was formulated in the 20th century—and in the case of quantum-mechanical calculations we have to use many, often coarse, approximations. Even in idealized solid states, such as ideal monocrystalline structures, exact quantum-mechanical calculations are practically impossible. In semi-conductor lasers, slightly more complex structures (heterostructures) are used, which require additional approximations. Fortunately, semiconductor lasers are very useful devices of which many different types are therefore made, providing extensive experimental data which can be used to verify the proposed simplifications. Moreover, semiconductor laser technology is closely related to other important research areas such as single photon emitters, entangled states and Bose-Einstein condensation—providing further motivation to conduct investigations and another source of experimental observations.

The papers include quantum-mechanical calculations for different types of heterostructure (quantum wells, quantum dots and superlattices), as well as algorithms used in real numerical calculations with convergence analysis. I also present constructions in which I have been involved (electrically and optically pumped lasers, edge-emitting, surface-emitting, external cavity diode lasers, quantum cascade lasers), which have been fabricated or are planned to be made in the near future. Naturally, the models used for such different con-

structions vary significantly, but the underlying physics is the same, and many of their elements are interchangeable.

My work on the modeling of semiconductor lasers has been part of the activity of the Photonics Group at the Institute of Physics, Lodz University of Technology, led by Prof. Włodzimierz Nakwaski, and could not have been completed without the help and inspiration of my colleagues, who produced individual models which were then developed and joined together to form a general model. Our work has also benefitted from partnerships with the Institute of Electron Technology in Warsaw, the Laboratory of Physics of Nanostructures at the École polytechnique fédérale de Lausanne, and with the Division of Microelectronics at Nanyang Technological University in Singapore. I personally was able to gain experience working in experimental laboratories at the first two of these institutions, developing knowledge and expertise which have been extremely useful, including in my theoretical investigations.

2. Tunnelling of carriers in multiple quantum wells [1]

In 1962, three independent publications on semiconductor lasers appeared [13–15]. The active regions were simple p-n junctions. They operated only at the temperature of liquid nitrogen and in pulsed mode, and had threshold current densities of over $10^4\,\mathrm{A/cm^2}$. These shortcomings were due to a lack of optical confinement of the modes, as well as to a lack of confinement of the electrons and holes. Soon, however, lasers with a double heterostructure (DHS) appeared, in which a narrower-gap material (which functions as both the waveguide and the active region) is surrounded by a wider-gap material. In this design, both the mode and the carriers are confined. The first laser to emit a continuous wave at room temperature, driven by current with a density of around $2000\,\mathrm{A/cm^2}$ was constructed in 1970 [16].

The next breakthrough was achieved by splitting the optical confinement (the minimal thickness of which is determined by the wavelength) and the confinement for the carriers, which it is beneficial to reduce, in order to increase the carrier density. Such designs were called *separate confinement heterostructures* (SCHs). When the thickness of the active region (i.e. the material with the lowest band gap) is in the order of nanometers, quantum effects, beneficial in this case, appear. In bulk material, the density of states is proportional to the square root of kinetic energy. This means that the density of the carriers that contribute to population inversion—that is, those with the least energy—is very low, since $\sqrt{E} \to 0$ when $E \to 0$ (see figure 1, 3D curve). If the carriers are spatially confined in one dimension within a region the width of a few nanometers, momentum in that direction is quantized. The momentum cannot be zero, so the minimal kinetic energy must be greater than zero. This implies that the density of states at the minimal energy is no longer 0 (see figure 1). Such structures are called *quantum wells* (QWs). Quantum-well lasers appeared in the late 1970s [17] and enabled a reduction of threshold current densities to the order of $100\,\mathrm{A/cm^2}$.

Reducing the thickness of the active layer also causes the volume at which the laser radiation is amplified to be reduced. This is especially important in vertical-cavity lasers (i.e. lasers in which the direction of the emission is perpendicular to the epitaxial layers). If, due to this effect, the gain provided by a single quantum well is insufficient, multiple quantum well (MQW) active regions can be used, consisting of several quantum wells separated by thin barriers. These barriers must be thin enough to make the whole active region

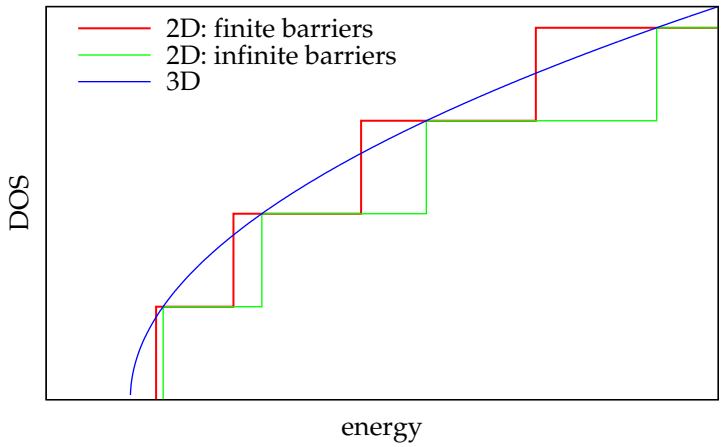

Figure 1. Two- and three-dimensional densities of states (DOS). In real structures of quantum-well lasers the barriers cannot be considered infinite.

narrow relative to the wavelength. If, on the other hand, the barriers are too thin, the wells interact strongly, reducing the beneficial effects of the spatial confinement of the carriers.

In structures containing MWQs, the uniformity of the population of wells becomes an issue. If the whole system was isolated with a well-defined temperature, this problem would not exist, because such systems would be populated by electrons according to the Fermi-Dirac distribution. However, in a system into which new carriers are delivered while others disappear, a certain degree of localisation is possible. This effect is reduced by decoherence processes and by the fact that localised states are unstable, i.e. a localised particle will tunnel between the wells. In a paper published in 2009 [1], I estimated the time needed by a localised electron to tunnel from one side of a system of identical wells (typical for semiconductor lasers) to the opposite side, and then compared this time with the average lifetime of the carrier in the laser. What now follows is a summary of this paper and its main contributions.

The most general description of a quantum state is the density matrix. By constructing this matrix for a system of identical quantum wells and solving the evolution equation, the following formula was calculated for the expected value of the position of a particle as a function of time:

$$\langle \hat{z} \rangle (t) = \sum_{n<m} a_{nm} \cos(\omega_{nm} t) \tag{1}$$

$$\omega_{nm} = \frac{E_m - E_n}{\hbar} \tag{2}$$

where E_i is the i-th (counting from the bottom) energy level (1-dimensional Schrödinger equation eigenstates are not degenerated, so $\omega_{nm} \neq 0$), while a_{nm} are certain coefficients. The time of tunnelling τ_t can be estimated as the time after which the most slowly varying term changes its sign into its opposite:

$$\tau_t \leqslant \frac{\pi\hbar}{\min\limits_{n<m}(E_m - E_n)} \tag{3}$$

The minimal difference needed between energy levels can be found numerically, since calculating the levels themselves requires numerical calculation. However, an interesting approximation can also be found analytically, which enables the important parameters to be identified and their influence on this difference to be determined qualitatively.

The energy levels of a Hamiltonian describing a system consisting of wells separated by barriers can be calculated as zeros of the determinant of a matrix of which the elements depend on energy. The matrix for a system of n wells is almost block-diagonal, i.e. only a very few elements do not fit this scheme. The matrices on the main diagonal are the matrices of a system with a single well. As a result, it was possible to find a recursive formula for the determinant of the matrix for an arbitrary number of identical wells separated by identical barriers. Eventually, a function of energy $W_n(\mathcal{E})$ which is a polynomial of the n-th degree (n being the number of wells) of variable $W_1(\mathcal{E})$ (i.e. the determinant of the single-well matrix) was found, which allows solutions of the equation $W_n(\mathcal{E}) = 0$ to be expressed as corrections to the solutions of the equation $W_1(\mathcal{E}) = 0$, which are the energy levels for a system with a single well. Very close agreement was found when the results obtained using this method were compared with the exact values (found numerically) for two- and four-well systems.

Following this analytic approach, interesting formulas can be obtained. For example, in a system of two or four wells, where the depth of the wells (U_0) is large compared to the lowest energy level (δE), the distance between the closest levels is proportional to:

$$\delta E \exp\left(-2d\frac{\sqrt{2m_b(U_0-\delta E)}}{\hbar}\right) \tag{4}$$

where $2d$ is the barrier width and m_b is the effective mass of the carrier in the barriers. The time of tunnelling estimated by formula (3) for an electron in a system of two quantum wells with widths of 60 Å, separated by 70 Å-wide barriers, and with other parameters similar to those in the arsenide materials, is less than 1 ps. As might be expected, for such systems with four quantum wells the time of tunnelling is slightly more than twice as long. It is worth emphasizing that this is the longest time of tunnelling, and applies to the electrons at the bottom of the quantum wells. Electrons with higher energies tunnel much faster.

3. Above-threshold model [2, 3]

Lasers can be optimised in terms of many different parameters. Naturally, the most fundamental question is whether or not the laser will lase, i.e. whether the laser will reach the threshold. In most cases, the lower the threshold (usually expressed as the threshold current) the better. However, a construction optimised to have the lowest possible threshold current is not necessarily optimal in terms of such important parameters as efficiency, maximal output power, and single- or multi-mode operation. A model which can describe the laser above its threshold, and allows us to calculate how the emitted power depends on the current (the so called light-current curve), is called an over-threshold model.

An over-threshold model has to take into account stimulated emission as an additional source of carrier losses in the active region. The losses caused by stimulated emission are proportional to the product of the light intensity and the material gain. Because of the non-linear dependence of the gain on carrier concentration, these losses introduce a highly

non-linear term to the diffusion equation, which may cause problems with its numerical solution.

In a paper published in *Physica E* [2], the convergence of the diffusion equation in the threshold (or below threshold) case was analysed and found to have the following form:

$$\kappa\Delta u(\boldsymbol{r}) - \big(Au(\boldsymbol{r}) + Bu^2(\boldsymbol{r}) + Cu^3(\boldsymbol{r})\big) + \frac{j_\perp(\boldsymbol{r})}{ed} = 0 \tag{5}$$

where u is carrier concentration, $\boldsymbol{r}$ is position in the plane of the active region, and A, B, C are the standard constants (independent of u, although they may depend on $\boldsymbol{r}$), which describe the carrier recombination processes (but not the stimulated emission). The current density perpendicular to the active region is denoted by $j_\perp$, e is is the elementary charge and d the thickness of the active region. This equation describes how the carriers injected into the quantum well diffuse and recombine. Coefficient A describes the rate of the monomolecular recombination (i.e. recombination on defects), B is the coefficient of the bimolecular recombination (i.e. spontaneous emission) and C is the Auger recombination coefficient. The solution of this equation gives the distribution of carrier concentration in the active region, which in turn allows us to find the distribution of the optical gain.

Numerical methods such as the finite element method are very effective at solving linear differential equations. For this reason, the solution (or more precisely, an approximated solution) of a nonlinear equation can be obtained by iterative solving of appropriately linearized equations. In the threshold case, the only problems are the terms Bu^2 and Cu^3. These terms can be linearized using the first order Taylor polynomial calculated at u_0—the value of the concentration taken from the previous iteration. This leads to a linear equation with the following form:

$$\kappa\Delta u - (u - u_0)\frac{\partial L}{\partial u}(u_0) - L(u_0) + \frac{j_\perp}{ed} = 0 \tag{6}$$

where

$$L(u) = Au + Bu^2 + Cu^3 \tag{7}$$

is the function that describes carrier losses. After a simple calculation of the derivative of the threshold losses described by the formula (7), the following formula was found:

$$\kappa\Delta u - (A + 2Bu_0 + 3Cu_0^2)u + \frac{j_\perp}{ed} + Bu_0^2 + 2Cu_0^3 = 0 \tag{8}$$

The fundamental question is of course whether this method is convergent. To prove convergence, the equations for two adjacent iterations were subtracted. Using the mean value theorem, the following equation for δ_i (the difference of the concentrations calculated in the adjacent iterations) was obtained:

$$\delta_i = -(u_i - u_{i-1}) \tag{9}$$

$$\kappa\Delta\delta_i - \delta_i\frac{\partial L}{\partial u}(u_{i-1}) + \varrho_i\delta_{i-1}^2\frac{\partial^2 L}{\partial u^2}(\mu_i) = 0 \tag{10}$$

where q_i is a function with values from the interval $(0, 1)$ and μ_i is a function with values between u_{i-1} and u_{i-2}. In the threshold case, equation (10) has the following form:

$$\kappa\Delta\delta_i - \delta_i(A + 2Bu_{i-1} + 3Cu_{i-1}^2) + \varrho_i\delta_{i-1}^2(2B + 6C\mu_i) = 0 \tag{11}$$

Formally, this equation has the form of a diffusion equation (with the unknown function δ_i) with losses proportional to δ_i and non-negative sources independent on δ_i. This means that δ_i as the solution of this equation is non-negative. So, according to the definition (9), the sequence of concentration u_i is non-increasing (for $i \geqslant 2$). On the other hand, this sequence is bounded from below by 0 (because concentration must be non-negative) and so the sequence is convergent.

In the over-threshold case, the carrier losses caused by stimulated emission must be included. To the threshold losses L described by equation (7) one must add, in the case of single-mode operation, an appropriate term:

$$L_{\mathrm{ot}}(\boldsymbol{r}) = L(\boldsymbol{r}) + P\frac{2gM(\boldsymbol{r})}{(1-R)\hbar\omega \int_S M} \tag{12}$$

where P is the emitted power, R is the reflectivity of the mirror through which the radiation is emitted (the other is assumed to have 100% reflectivity), $M(\boldsymbol{r})/\int_S M$ is the normalised transverse mode distribution and $\hbar\omega$ is the photon energy. Finding the unknown power P for a given voltage U (higher than the threshold voltage) relies on solving a system of equations formed by the diffusion equation and an optical model which will show when the gain has compensated for all radiation losses.

The approach which led to equation (10) can also be used in the over-threshold case. Similarly to the threshold case, function $\partial L/\partial u$ is also positive, so if the second derivative $\partial^2 L/\partial u^2$ is positive, we can also be sure, in this case, that the sequence of iterations will be convergent. Unfortunately, function $\partial^2 g/\partial u^2$ is negative, so at higher powers this condition may be not fulfilled.

In the case of multi-mode operation, equation (12) is modified by adding all the lasing transverse modes:

$$L_{\mathrm{ot}} = L + \sum_i P_i \frac{2g_i M_i}{(1-R_i)\hbar\omega_i \int_S M_i} \tag{13}$$

where index i numerates the lasing modes. The additional equations which allow us to find the powers P_i (powers of all the modes) are the conditions which state that the modal gain for each of the modes must be 0.

The model described above does not require in its over-threshold part any additional parameters to those used in the threshold case. Figure 2 presents results of over-threshold modelling compared with corresponding experimental data obtained for the VCSEL described in paper [18]. A very good agreement will be noticed between the model and the experiment. Competition between the fundamental mode (LP_{01}) and the first excited higher-order mode (LP_{11}) is also visible in the calculations.

The results presented in paper [2] were included in the model of semiconductor lasers developed by our group and have been used, with a significantly larger scope in the modelling and optimisation of different constructions with a significantly larger scope.

4. Quantum cascade lasers and superlattices [4, 5]

Quantum cascade lasers (QCLs) differ from other semiconductor lasers in many ways. The most fundamental of these is the lack of a p-n (or more precisely p-i-n) junction, which in

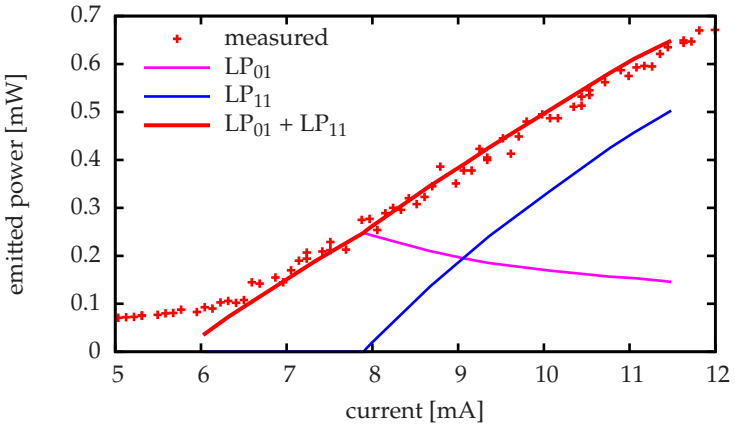

Figure 2. Calculated and measured light-current curves for the VCSEL described in [18]. The lines LP_{01} i LP_{11} are the powers of the corresponding transverse modes.

other light-emitting semiconductor devices is the source of photons. The wavelengths at which QCLs emit are in the mid- and far-infrared ranges, where small and effective emitters are difficult to obtain. The creators of the first QCL, at Bell Laboratories, published their results in a series articles in 1994 [19–22]. Their laser was fabricated on InP substrate and the wells and barriers in the active region were made from InGaAs/InAlAs. A significant advantage of this material system is the fact that InP has a lower refractive index in relation to the active region which, as a result, becomes a waveguide. In QCLs with AlGaAs/GaAs active regions grown on GaAs substrates, in which the active region has a lower refractive index, the substrate must be optically insulated from the active region, which is a significant disadvantage [23]. Such lasers appeared a few years later [24, 25] and in Poland were fabricated for the first time at the Institute of Electron Technology in Warsaw in 2009 [26].

The radiative transitions in QCLs take place between states located within a single band (in practice, the conduction band). Figure 3 gives a schematic view of the difference between inter- and intra-band transitions. In a single-QW potential, such as that shown in this figure, it is not possible to obtain population inversion. A suitable scheme of quantum states can be obtained in a superlattice, i.e. a periodic system of thin barriers and wells, polarised using an appropriate electric field. In each of the periods of the superlattice, there is a part containing states in which population inversion may appear and a part responsible for the transport of electrons from one lasing part to the next, in the adjacent period of the superlattice (figure 4). In this way, a quantum cascade of light-emitting electrons is formed, and for this reason such lasers are called *quantum-cascade lasers*. The energy levels and their wave functions must be designed in such a way that certain levels are very effectively depopulated in non-radiative processes, while in others radiative recombination is more effective.

In papers concerning the electronic structure of superlattices [5, 26], the envelope function approximation was used to find electronic states in such superlattices. This method had been widely used on similar problems, although in the case of quantum cascade lasers the layers might be only a few atomic monolayers thick. Ordinarily, the method assumes that the envelope function is almost constant at inter-atomic distances. Even so,

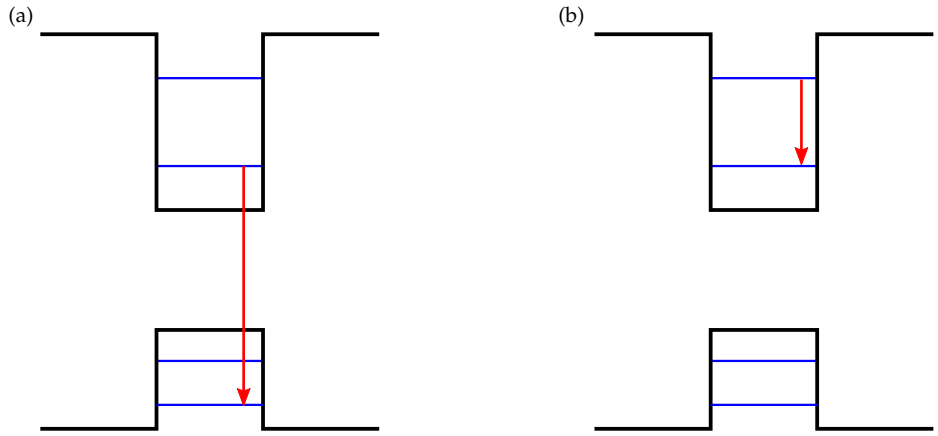

Figure 3. Transitions between states in quantum wells, represented by red arrows: inter-band (a) and intra-band (b).

it worked surprisingly well, i.e. its predictions agreed with the experiment, and required only 1-dimensional calculations. The envelope functions in such superlattices are solutions of the Schrödinger equation with a potential as in figure 5 and effective electron masses. In order to avoid problems with unbound states, an infinite barrier was placed next to one end of the superlattice potential. In addition, the effective masses in the barriers and wells were different. At the interfaces the so-called Ben Daniel Duke conditions had to be fulfilled for each interface:

$$\lim_{z\to a^-} \Psi_i(z) = \lim_{z\to a^+} \Psi_{i+1}(z) \tag{14}$$

$$\lim_{z\to a^-} \frac{1}{m_i^*}\Psi_i'(z) = \lim_{z\to a^+} \frac{1}{m_{i+1}^*}\Psi_{i+1}'(z) \tag{15}$$

where a is the position of the interface, Ψ_i is the envelope function in the i-th layer and m_i^* is the effective mass in the i-th layer. Analytic solutions of the Schrödinger equation with potentials of constant electric fields $U(z) = eFz - U_0$ were known to be linear combinations of Airy's functions Ai and Bi:

$$\Phi(z) = A\mathrm{Ai}\big(k(Z_0 - z)\big) + B\mathrm{Bi}\big(k(Z_0 - z)\big) \tag{16}$$

$$k = \sqrt[3]{-\frac{2meF}{\hbar^2}} \qquad Z_0 = \frac{\mathcal{E} - U_0}{eF} \tag{17}$$

where $\mathcal{E}$ is an eigenenergy and $e < 0$ is the elementary charge. In order to find the energy levels and wave functions (or more precisely, the envelope functions) for the potential, as in figure 5, it was enough to join the analytic solutions (16) on the interfaces, using the conditions (14) and (15), and the boundary conditions. Non-zero solutions of this problem are possible only for certain values of parameter E, the energy levels. In the language of algebra, this means that we want to find non-zero solutions of the homogeneous system of $2n + 1$ linear equations (with the coefficients which depend on $\mathcal{E}$), where n is the number of the layers in the potential considered, and which have the same number of the unknowns (coefficients of the linear combination (16) in each layer). This system only has non-zero

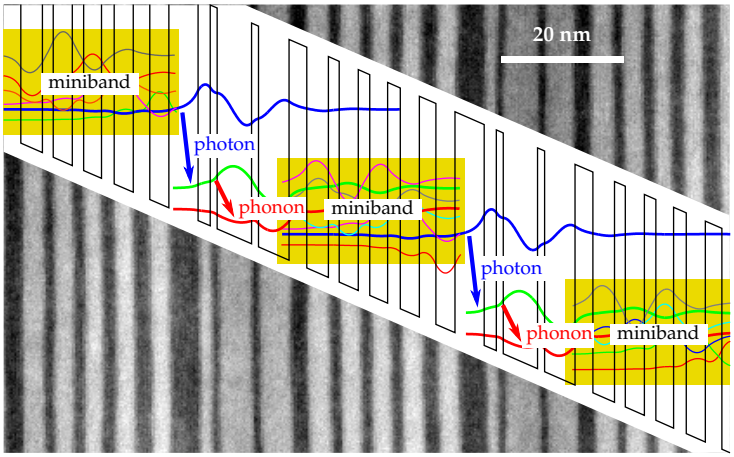

Figure 4. TEM image ([26]) of the layers that make up three periods of the superlattice of the laser described in [26] aligned with the picture of the potential in the conduction band with calculated wave functions of the most important quantum states.

solutions if the determinant of the matrix of the system is 0. Schematically, the matrix takes the form presented in formula (18), where the non-zero entries are denoted by bullets.

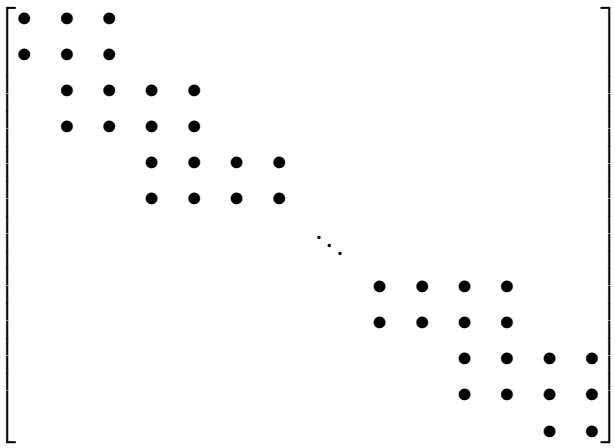

(18)

This matrix is not symmetrical, which makes finding the energy levels more difficult. For that purpose, singular value decomposition (SVD) was used, which exists for any matrix and allows the matrix $\mathbf{M}$ to be written as the following product:

$$\mathbf{M} = \mathbf{U}\mathbf{\Sigma}\mathbf{V}^T \tag{19}$$

where matrices $\mathbf{U}$, $\mathbf{V}$ are unitary (and therefore non-singular), while the matrix $\mathbf{\Sigma}$ is diagonal and real. From this, we know that $\mathbf{M}$ is singular if and only if there is a zero on the diagonal of $\mathbf{\Sigma}$. A great advantage of this semi-analytic approach (which is not the only one available) is that it is possible to include the dependence of the effective mass on energy $\mathcal{E}$ (so-called band non-parabolicity) in the model. A Schrödinger equation in which the mass depends on energy is no longer a question of finding eigenvectors and eigenvalues for a linear operator,

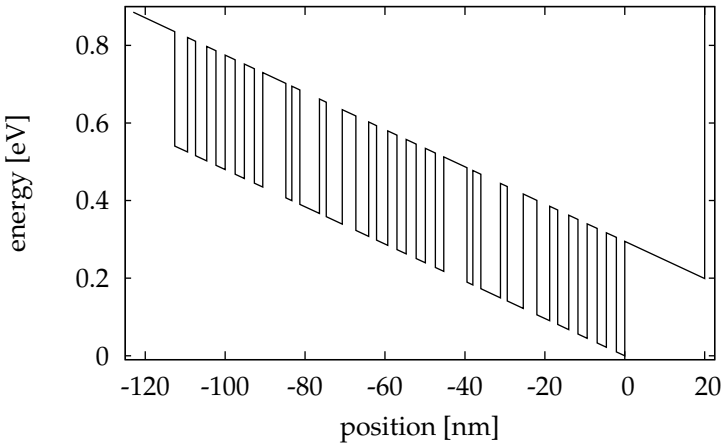

Figure 5. An example of potentials used in the calculations. It reproduces 2.5 periods of a QCL superlattice polarised by an electric field of 48 $\frac{\text{kV}}{\text{cm}}$. The infinite barrier is placed 20 nm from the edge of the superlattice.

so it is difficult to include this phenomenon in numerical methods that rely on discretisation and look for eigenvalues of matrices created this way.

It is very important fo find all of the energy levels. Numerical solving of equations with multiple solutions is always a problem. However, in this case, the states were non-degenerate (as bounded states of a 1-dimensional Schrödinger equation) and the number of zeros of the l-th wave function was l (when the functions were numbered from 0 counting from the lowest energy). In practice, this greatly facilitated the finding of solutions, especially as the number of zeros in a wave function can be calculated in a smart way, without requiring the wave function values inside the layers to be mapped.

4.1. Applications of the model

GaAs-based QCLs were produced as part of the project "Advanced technologies for infrared photonics" at the Institute of Electron Technology. The fabrication of the actual lasers was preceded by calibration growths of test superlattices, measurements and calculations. Each test superlattice was a multiple repetition of a well-barrier pair and was not polarised. In such superlattices, mini-bands are formed in which the energy levels are densely packed. This presents a problem when attempts are made to find the zeros numerically, since numerical errors can make distinctions between close levels impossible. The thicknesses of the mini-bands are determined mainly by the width of the barriers.

The structures our group investigated had barriers with thicknesses of 46 Å and 11 Å. Calculations showed that for barriers with a thickness of 46 Å the mini-bands are so narrow that it is difficult to distinguish them on a spectrum from the energy levels of a single-well. However, when the barriers are 11 Å wide, even though the heavy-hole mini-bands are still narrow, the electron and light-hole mini-bands are around 30 meV wide. This creates a qualitative change in the measured photoluminescence spectra. Moreover, the calculations revealed certain discrepancies between the design and the fabricated structures in terms

of the composition and thickness of the layers. These findings were confirmed in other experiments.

Photoluminescence spectra give little information concerning higher energy levels. Much more can deduced from analysis of photoreflectance spectra. This type of experiment was performed at the Institute of Physics, Wrocław University of Technology. Analysis of the spectra obtained seems to confirm quantitative agreement between the calculations and reality, but the fact that interpretation of photoreflectance spectra is sometimes ambiguous must be taken into account. A very valuable confirmation of the photoreflectance results was provided by a direct measurement of inter-band photoluminescence, i.e. the emission caused by transitions of electrons between two minibands in the conduction band. The agreement between the calculated transmission energy and that measured in our experiments was found to be very good—the discrepancy was less than 10% in the worst case.

Superlattices in active regions of QCLs are much more complicated than the test structures mentioned above. After a few corrections to the growth and processing of the laser structures, at the Institute of Electron Technology in Warsaw, on Friday 13th of February 2009 at around 13 UTC, the first Polish QCL lased [26]. The work summarized here includes my involvement in investigations that contributed this project, alongside research teams and in collaboration with Polish laboratories.

5. Quanum dot lasers [6]

The idea of using 0-dimensional structures (i.e. objects with very small dimensions in all three directions) in semiconductor lasers appeared in the early 1980s [27], shortly after the first such structures were fabricated, in the Soviet Union in 1981 [28] (Russian original), [29] (English translation). At that time, it was not possible to use 0-dimensional structures in real lasers, but theory predicted that such lasers would have very low threshold currents regardless of temperature. The models described the objects as cuboids (or often as cubes), which were called *quantum boxes*. The first publications on semiconductor lasers in which emission originated in quantum dots (the term *quantum dot* was already in use), appeared in 1994 [30], although, because of the low quality of the dots, this observation was questioned [31]. In spite of progress in the technology, quantum dots in the active regions of semiconductor lasers are still far from reaching the parameters described in ideal models. This is one of the reasons why the characteristics of actual lasers differ significantly from the original predictions.

The most important feature of the quantum dot (generally defined as a potential bounded in all three dimensions) is its discrete energy spectrum, which is similar to the spectra in atoms. Unlike in atoms, however, the discrete part of the spectrum is relatively narrow—below the potential of the barrier material. Even so, from the point of view of basic research, an advantage of quantum dots is the fact they are stationary and can be investigated individually—which, in the case of atoms, is very difficult. In laser applications, the discrete spectrum means that creating population inversion in quantum dots requires significantly fewer carriers than the same operation would in quantum wells. This enables the fabrication of lasers with extremely low threshold currents [32–35]. Moreover, thanks to different fabrication technologies, it is possible to achieve emission in spectral ranges which are out of the reach of quantum wells based on similar materials [36–38]. Optical

amplifiers based on quantum dots are very fast and can have wide gain spectra [39]. Similar features make quantum dots very good absorbers in semiconductor saturable absorber mirrors (SESAMs) [40].

Different kinds of quantum dot are now manufactured, depending on their applications. For basic research, they are very convenient, immobile analogues of atoms which, moreover, can sometimes be excited electrically. Because of this, they are also a very useful tool which can be designed to emit single photons, generating entangled states, and can be used for other applications in experiments concerning the most fundamental questions in physics [41–44]. For such uses, single dots or pairs of coupled dots are normally used. Lasers, however, need active regions with a very high surface density of dots. Unfortunately, contemporary methods of growing quantum-dot active regions are not able to create layers where dots are at once identical (or almost identical) and highly numerous. Because of the stochastic distribution of the dimensions of dots, the spectrum of the whole system no longer resemble an atomic spectrum and becomes a continuous spectrum. For this reason, when considering quantum dot lasers it is not necessary to construct a very precise model of individual dots. It is enough to describe the average density of states over the whole system of dots.

Models of step-like potentials, which work well for quantum wells, might suggest that the distances between successive energy levels should increase. However, experiments with self-organising quantum dots, for instance in Stranski-Krastanov growth mode (such processes are usually used for the growth of laser structures), show that the distances between the subsequent photoluminescence peaks are almost identical [45, 46]. For this rea-

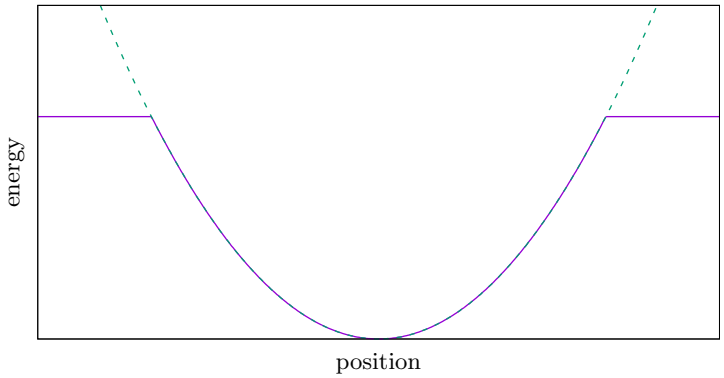

Figure 6. Potential of a harmonic oscillator (dashed line—parabola) and a model of quantum-dot potential (continuous line).

son, a 2-dimensional harmonic oscillator potential is often used. The third dimension is taken into account as a shift of the energy levels in the 2D potential. Additional theoretical investigation has proven the workability of this simplified model [47, 48]. The growth direction in which the dot is flattened compared with the other two dimensions is treated separately. The potential inside the dot cannot be unbounded, as is the case in harmonic oscillator potentials, since it is limited by the barrier potentials. A simple modification of the harmonic potential, presented in figure 6, can avoid this problem. The solution

of the Schrödinger's equation for such a potential is much more complicated than using well-known analytic solutions for harmonic oscillators. Fortunately, numerical calculations made for certain potentials show that the differences between the energy levels obtained in both potentials are negligible, which is not the case if one compares finite and infinite rectangular potential wells.

In order to calculate optical gain, it is necessary to know the potential profiles in the conduction and valence bands. The positions of photoluminescence peaks do not reveal all the necessary information. In the harmonic oscillator approximation, the energetic distance between the peaks is equal to $\hbar(\omega_c + \omega_v)$, and the distances between subsequent levels in the conduction and valence bands are $\hbar\omega_c$ i $\hbar\omega_v$, respectively. The photoluminescence spectrum determines the sum $\omega_c + \omega_v$, but to know both numbers one has to make an as sumption concerning the potentials. If we consider both potentials as being identical, we obtain the following relation:

$$\frac{\omega_c}{\omega_v} = \sqrt{\frac{m_v}{m_c}} \tag{20}$$

where m_c, m_h are the effective masses in the bands. Another possible assumption is that both potentials have the same width but different depths: U_c, U_v. In this case, a different relation holds:

$$\frac{\omega_c}{\omega_v} = \sqrt{\frac{m_v U_c}{m_c U_v}} \tag{21}$$

Assuming that the depths follow the same relation as in InGaAs/GaAs quantum wells, the relation $U_c/U_v \approx 7/3$ should be valid.

The degree of degeneracy of energy levels in the two-dimensional harmonic potential increases linearly with the number of the level. This means that under strong enough excitation the gain of the transitions between excited levels can be higher than that of the base-level transitions. This fact has important implications, to which we shall return.

The statistical parameters of a quantum-dot ensemble—such as surface density and full width at half maximum (FWHM) of the spectrum (which is determined by the variance of the distribution of the dot dimensions)—are crucial for the purposes of determining the laser properties. High surface density means that high gain can be obtained, but also that the carrier concentration needed to achieve transparency is higher. Similarly, good uniformity (i.e. low FWHM) increases the gain at the peak wavelength, but decreases the tolerance upon detuning from the peak.

In edge-emitting lasers, the longitudinal modes are so densely distributed that the emitted wavelength fits with the gain maximum. Switching to the shorter wavelength, related with excited-state transmission, is therefore a problem (or in other respects an opportunity) [49, 50]. On one hand, it is difficult to achieve high-power emission at the long wavelength, corresponding to ground-level emission. On the other hand, an important advantage of quantum-dot lasers is the fact that their threshold current is usually very low [32–35]. In vertical cavity surface emitting lasers, much higher material gains and wider gain spectra are necessary. These lasers operate in a single longitudinal mode, determined by a very short resonator. As the temperature rises due to the electrical current, the gain peak shifts more strongly than the resonator wavelength. For this reason, in order to achieve higher powers, the structures are usually designed in such a way that at the threshold the laser operates at a wavelength longer than the gain peak wavelength. As a result, the gain

improves with the increasing current. The threshold current is increased by such detuning, so designs must be made carefully. In VCSELs, both the surface dot density and the uniformity of the dots have a strong, often non-monotonic, impact on the parameters of the device (see figure 7). Paper [6] shows numerous relations illustrating this influence, both for tuned and detuned lasers. In particular, it suggests that (up to a certain point) lowering the level of dot uniformity does not increase the threshold (see figure 7). The results and

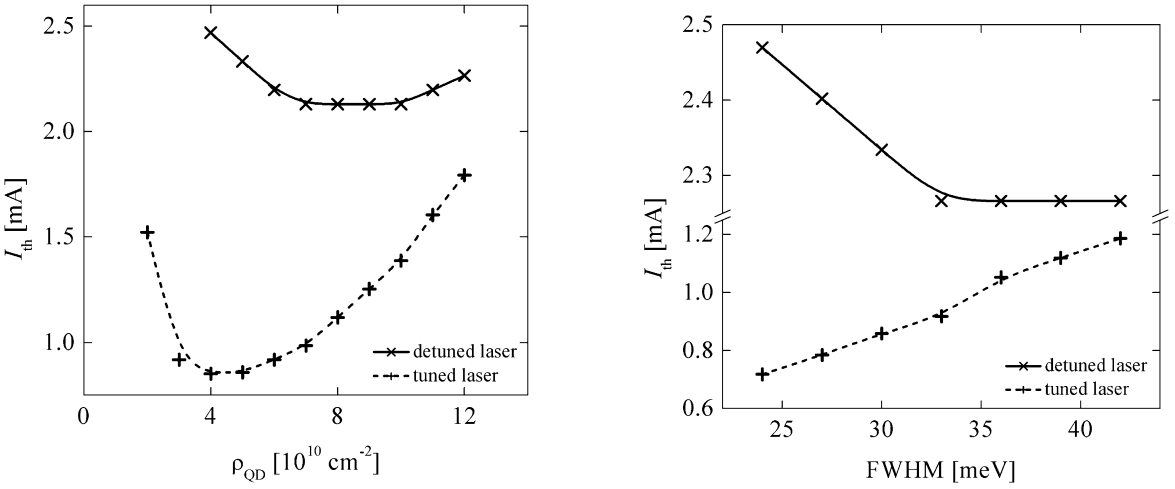

Figure 7. Threshold current density as a function of surface density of QDs (left) and QD uniformity (right). Details can be found in [6].

models presented here have been used to fabricate quantum-dot VCSELs [18, 51]. In this type of laser, its active region has to provide a high optical gain, what makes the application of quantum dots especially difficult.

This could be helpful in obtaining higher powers from quantum dot VCSELs. The research presented here shows that quantum-dot based active regions have many advantages, but also important limitations. These limitations may be some of the reasons why quantum dots have not replaced quantum wells in most applications.

6. Vertical external cavity surface emitting laser [7, 8]

Semiconductor lasers are in general electrically-pumped devices, and this is perhaps their principal advantage, together with their very small size and remarkable efficiency. However, *vertical external cavity surface emitting lasers* (VECSELs), sometimes called semiconductor disc lasers (which is the more general term), are for the most part optically pumped. Schematic views of one such laser are given in figure 8. Typical semiconductor lasers emit either high power (edge-emitting lasers) or good-quality beams (VCSELs). With optical pumping, it is possible to have both features at the same time. Optical pumping is usually performed by a high-power semiconductor laser, so the VECSEL can be seen as a converter in which a high-power but low-quality beam becomes a very high-quality beam, still with high power (although of course lower than that of the pump) [52]. This is not, however, the only or maybe even the most important application of VECSELs. The external cavity can

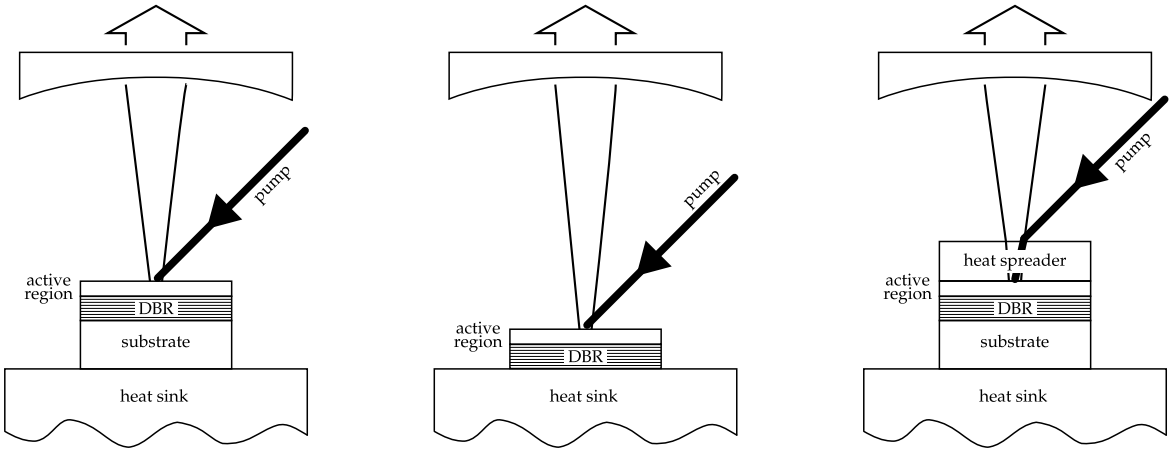

(a) Basic (*as grown*) structure capable of yielding only limited powers

(b) Structure with the substrate removed (*flip-chip*)

(c) Structure with an intra-cavity heat spreader made from a transparent heat conducting material

Figure 8. Schemes of three typical VECSEL structures. Scale and aspect ratio are not preserved (the thickness of the DBR and active region are only a few micrometers, whereas the substrate and heat spreader are a few hundreds of microns thick). The cavity is formed by the DBR and external concave mirror.

contain a non-linear crystal or saturable absorber and, thanks to the very high field intensity within the cavity, spectacular effects can be achieved.

The first articles about such lasers were published in the early 1990s [53]. The highest recorded power from a single-chip VECSEL now exceeds 100 W at CW [54]. By second harmonic generation, it is possible to obtain very high, multi-watt powers [55, 56], which are often impossible to achieve with other semiconductor lasers at these wavelengths. A good review of VECSELs can be found here [57]. Our group is involved in works on VECSELs emitting in a spectral range of 1300–1550 nm [58], near 1 µm [59, 60], and generating the second harmonic in the visible spectrum [61].

The power of the pumping laser must be greater than the emitted power. The efficiency of VECSELs can be close to 50% [62], but even so the amount of pumping power that dissipates as heat is very high. In the case of the simplest construction, presented in figure 8(a), the heat must flow through the whole thick substrate. If we assume that the diameter of the area through which the heat flows is 200 µm (this is the order of pumping beam diameters) and the thickness of the substrate (GaAs) is 400 µm, we obtain a temperature difference between the top and bottom of the substrate of almost 300 K per Watt of heat. Of course, the diameter of the cylinder through which the heat is transported is not well-defined, but

this coarse approximation is not too inaccurate. Under such conditions, it is not possible to build a satisfactory laser, but this simple estimation suggests two possible ways in which the thermal resistance of the structure may be reduced:

1. by reducing the distance between the most heated part of the structure and the heat sink
2. by broadening the area through which heat is transported to the heat sink

The first method can be achieved simply (at least in theory) by removing or significantly thinning the substrate, as shown in figure 8(b). As for the second, it is not sufficient to increase the pumping spot, since a certain threshold power density is necessary, so the threshold power (which turns almost entirely into heat) would increase with the spot area. Fortunately, there is another way of increasing the width of the heat stream flowing into the substrate. By placing a thick layer of a material of good thermal conductivity on or beneath the heated area, it is possible to make the heat spread out laterally within this layer, and the heat flows down to the heat sink in a much wider stream, reducing thermal resistance. Because of this mechanism, the additional layer is called a *heat spreader*. Figure 8(c) presents a structure with a heat spreader over the active region (inside the optical cavity). Alternatively, the spreader can be placed between the active region and the heat sink. It is important to place the heat spreader as close as possible to the main heat source, which in this case is on top of the active region. However, the intra-cavity layer can introduce unwanted optical imperfections in the cavity, so both schemes (heat spreader over and under the laser structure) are used.

When an intra-cavity heat spreader is used, it is crucial that it be transparent for both the light from the pump and the light emitted by the VECSEL. However, the choice of transparent materials which are also good heat conductors is rather limited. Fortunately, the best known heat conductor—diamond—is transparent. Another candidate is silicon carbide, although this is not only rather expensive and not readily available, but is inferior to diamond in terms of its thermal properties. It is also important to ensure the quality of the surfaces of both materials which are in contact with each other. Especially in the case of intra-cavity heat spreaders, the contact between the heat spreader and the laser chip must be as good as possible, since any additional heat resistance at their interface deteriorates the performance of the heat spreader. The other (upper) surface of the heat spreader must also be of good quality, since scattering of the emitted light can introduce significant optical losses. For these reasons, the quality of all surfaces should be very high [63].

Both methods of reducing heat resistance (application of a heat spreader and removing the substrate) can be used simultaneously. However, there is a question over which method is more effective, and whether there is any benefit to using them together. Three-dimensional calculations of heat transfer in VECSELs performed using software developed by our group, produced some interesting results. Under the assumption that the lateral distribution of the heat sources is described by the Gaussian distribution of the standard deviation 50 µm (which translates as a diameter of 200 µm using the $1/e^2$ definition) and the total power is 4 W, we performed calculations for:

1. a structure without the substrate and heat spreader (as in figure 8(b))
2. a structure with a substrate of thickness 100 µm (i.e. a thinned substrate) and a diamond heat spreader (figure 8(c)). The diamond's heat conductivity was assumed to be equal to

1200 $\frac{\mathrm{W}}{\mathrm{mK}}$, which is much less than the highest reported values, while the contact between the surfaces was assumed to be ideal
3. a combination of the two aforementioned structures

The first structure was found to have the highest thermal resistance (24.5 K/W). However, it was many times lower than in the as-grown structure. The thermal resistance of structure number 2 was more than four times lower than in structure number one. The optimal structure, of course, was the third, which had a thermal resistance slightly over 4 K/W. Despite the fact that these calculations did not take into account the resistances of the chip–the heat spreader interface and the heat sink–chip interface (solder)—which are very important but difficult to measure, it is clear that heat spreaders have great potential.

6.1. High contrast grating

In each of the structures in figure 8, the DBR presents an obstacle to the heat as it travels towards the heat sink. The thickness of the DBR is determined by the parameters of its materials and by the requirement for high reflectivity ($\gtrapprox$ 99%). The DBR makes a very significant contribution to the laser's thermal resistance, and if we could replace it with a superior heat conductor, this could allow for further optimisation of the VECSEL's properties.

There is another way to obtain very high reflectivities—a *high contrast grating* (HCG). In its most standard version, this is a periodic structure consisting of long stripes of high-refractive index material on a low-index material, which is sometimes deposited on a substrate with a high refractive index, as shown in figure 9. Such constructions are simi-

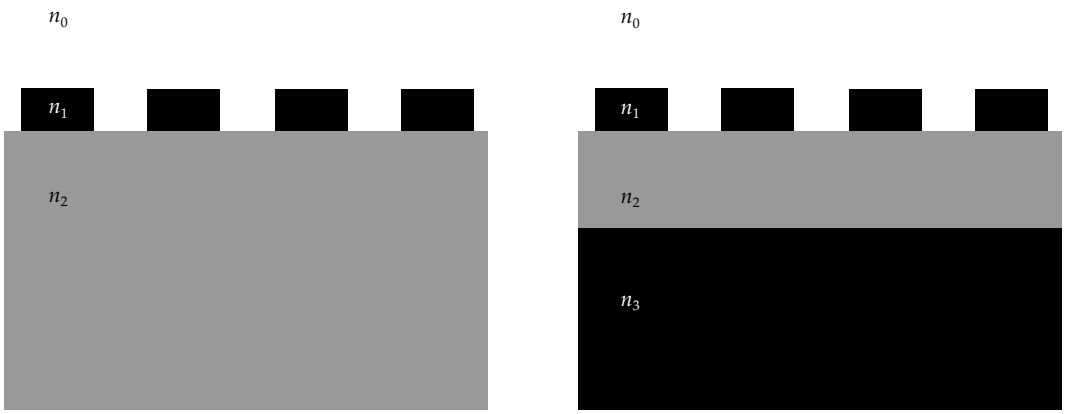

Figure 9. Schematic cross-sections of the two most common designs of high contrast grating. The refractive indices fulfil the following condition: $n_1, n_3 > n_0, n_2$. Usually the material with the lowest refractive index is air ($n_0 \approx 1$).

lar to a diffraction grating, but in this case the dimensions of the stripes and the distances between them are shorter than the wavelength. For this reason, the term *subwavelength high contrast grating* is sometimes used. The term 'high contrast' refers to the fact that there must be a clear difference between the refractive indices of the materials. By a careful combination of the dimensions and refractive indices, it is possible to obtain a reflectivity spectrum no worse than that in a DBR. From the point of view of thermal properties, it is then possible

to replace the thick DBR with, for instance, a diamond heat spreader with a silicon HCG structure. The high refractive index contrasts between the diamond, silicon and air produce very good optical properties in such structures.

Replacing the DBR with diamond should significantly reduce the laser's thermal resistance, but this is not the only advantage. In patent [**patent**] we analysed three structures:

1. a structure without the substrate and with a diamond intracavity heat spreader—the best that is currently available
2. a structure in which the DBR is replaced by a diamond with a silicon HCG structure inside the diamond
3. a structure in which the DBR is replaced by a diamond, and a hole is drilled into the copper heat sink in such a way that it should be possible to make an HCG on the diamond–air interface and insert an optical fibre from the bottom

The first structure is the reference. The second is the simplest (in terms of the concept, although not technically), only replacing the DBR with diamond. The calculated thermal resistance of the first structure is 4.84 K/W and of the second 3.54 K/W. The reduction is significant, but an HCG made of silicon surrounded by diamond has unsatisfactory optical properties—the reflectivity spectrum is too narrow. Moreover, the fabrication of such a structure would be difficult. Depositing silicon on diamond would seem to be a much

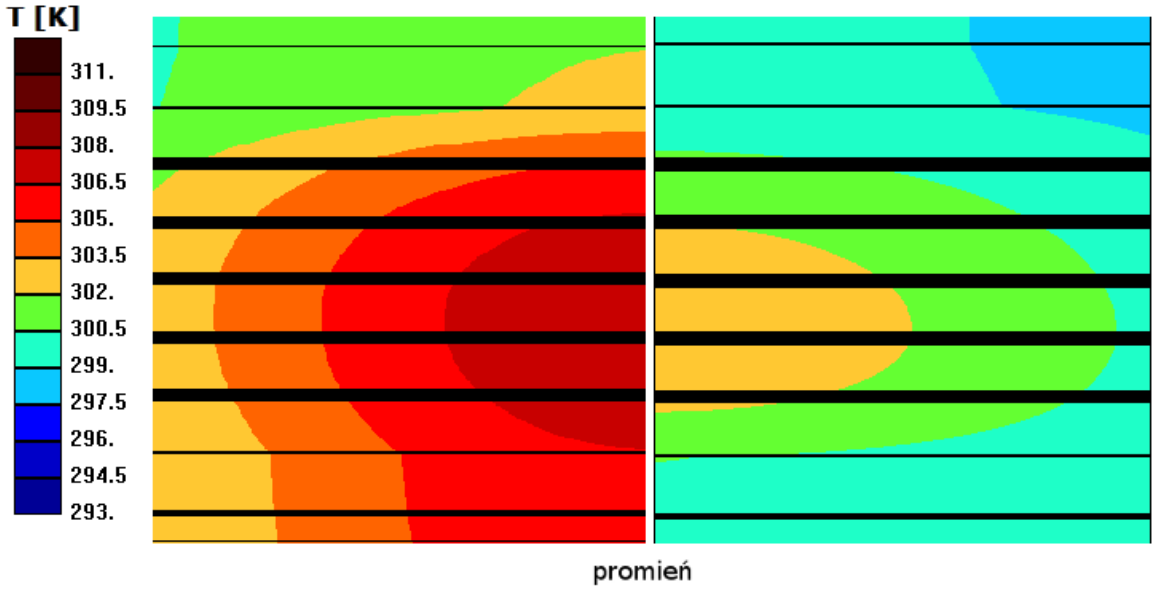

Figure 10. Comparison of temperature distributions in structure 1 (left) and 3 (right). The width of each of the presented sections is 100 µm.

better idea. The spectral width of reflectivity over 99.8% increases from 4 nm, in the case of structure two, to 60 nm. The maximal reflectivity is also higher, but in both structures it is very close to unity. Moreover, this method of fabrication is reasonably easy. The main problem is the air surrounding the HCG. It is required to obtain such good properties, but air is also a very good thermal insulator. On the bottom side of the laser, where such a

structure should be located, there is the heat sink, which must not be thermally insulated from the laser. Fortunately, thanks to the thick diamond between the HCG and the laser, which acts as a heat spreader, making a hole of 1 mm in diameter in the heat sink does not increase the thermal resistance of the device significantly—from 3.54 K/W to 3.69 K/W. Figure 10 shows the difference between the temperature distributions in the first structure (with a DBR on the bottom and diamond on top) and in the third (with diamond on both sides). The impact of the bottom diamond on heat transfer can clearly be seen. Due to the fact that we can make a hole in the heat sink along the laser's axis almost without affecting its thermal properties, it is possible to connect an optical fibre to the bottom. This would radically simplify the VECSEL's construction, and remove the necessity for precise adjustment of the pumping beam.

An HCG can also be designed to play many different roles. It seems possible to obtain almost perfect transparency, to create focusing mirrors of focal lengths of single microns, optical isolators, etc. HCGs are extensively investigated by our group, which has its confirmation in publications in influential journals and presentations at important conferences [64–69].

Whether or not VECSELs will find significant commercial applications beyond research laboratories is still an open question. One potentially important application is as light sources, if VECSELs prove to be superior in some respect to light sources based on more conventional emitters. Our group is involved in research on using VECSELs to produce visible light performed at the Institute of Electron Technology in Warsaw and École polytechnique fédérale de Lausanne, and some of the preliminary results have already been published [7, 61].

7. Model of capacitance in semiconductor lasers [9, 10]

Semiconductor lasers have multiple applications of which optical telecommunication is one of the most important. Contemporary long-distance data transmission systems are based mainly on distributed feedback (DFB) semiconductor lasers, which emit wavelengths of around 1550 nm. At short distances, such as between the chips of a computer or between computers in a building, copper wires are also becoming obsolete. Transmission of electrical signals has severe limitations [70, 71]. For example, electrical signals suffer from very high attenuation if the modulation frequency exceeds 1 GHz, while cross-talk between adjacent wires disturbs the signal. For these reasons, there is a need to replace copper wires by optical systems wherever a high bit rate is required. Replacing copper wires by optical links would help significantly to enhance the speed of high-performance computing (HPC) systems [70, 72]. Currently, optical links are deployed at the rack-to-rack and intra-rack scale [73]. Such optical links contain many elements, including light emitters. In short-distance links, emitters like those in long-distance systems cannot be used, for reasons including their cost, size, power consumption and temperature stability requirements. Distributed feedback lasers must be replaced by emitters suitable for short-distance systems. GaAs-based VCSELs are the natural choice, because of their low production costs and very low heat-to-bitrate-ratio [74]. In optical links, such lasers are driven by voltages modulated at frequencies of tens of GHz [75–81]. However, even small capacitance or inductance can introduce differences between the voltage and the current flowing through the laser. This

introduces a difference between the electrical signal (voltage) and the optical signal (intensity of the light emitted by the laser). making it difficult to distinguish logical low states from high states. This in turn can lead to errors in data optical transfer. In semiconductor lasers, not inductance but capacitance may be the problem, so capacitance has been analysed by many authors [76, 82–90]. However, our model is the first which can predict the properties of electrical modulation in semiconductor lasers.

The small signal modulation experiment (SSM) is the basic way to produce a quantitative description of the laser's reaction to modulation [91]. It allows to find $Z(f)$, which is the dependence of the laser's complex impedance on the modulation frequency. In the literature, many authors report fitting the values of resistances and capacitances in a relatively simple equivalent circuit to experimental results [80, 86, 87]. Such an approach gives an idea of the capacitances related to different elements of the laser, but cannot provide any information when a laser is being designed.

Our model, described in [9], is based on an analysis of constant-voltage potential distributions in a laser. These potential distributions are obtained by using the electrical and thermal models described earlier. The energy of the electric field can be used, instead of electric charge, to define the capacitance of a capacitor (C) by the following formula:

$$C = \frac{2\mathcal{E}}{U^2} \tag{22}$$

where E is the energy of the electric field and U is the voltage on the capacitor. An arbitrary area between two equipotential surfaces can be considered a capacitor. The energy of the electric filed in any area Ω can be calculated using the following formula:

$$\mathcal{E} = \frac{\varepsilon_0}{2} \int_\Omega \varepsilon(x,y,z) \big(\nabla V(x,y,z)\big)^2 \, dxdydz \tag{23}$$

where ε_0 is the vacuum permittivity, ε is the relative permittivity of the medium and V is the calculated potential distribution. Figure 11 presents an example of the distribu-

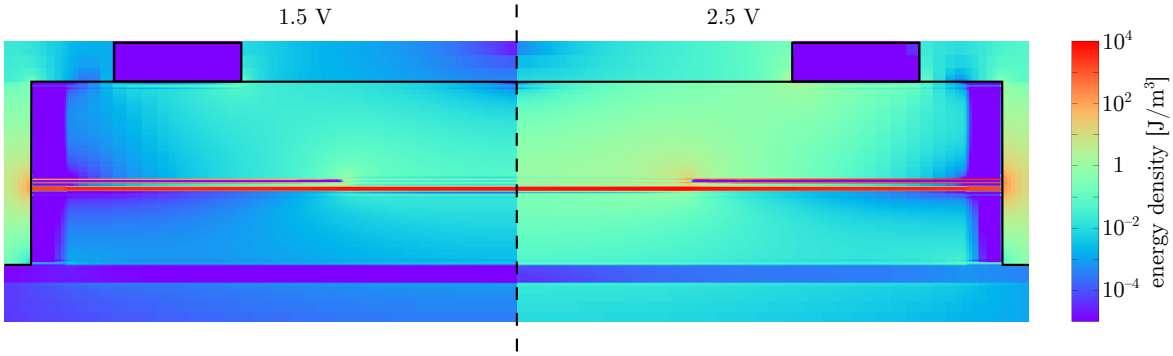

Figure 11. Distribution of the energy density of the electric field for two different voltages in a VCSEL structure [92]. The layers of high energy densities are (counting from bottom): the laser's junction and two oxide layers. The dashed line denotes the symmetry axis, common for both cross-sections.

tion of the electric field energy in an arsenide VCSEL designed for application in optical

links. Over 95% of the energy of the electric field is accumulated in the junction and two current-confining oxide layers. In order to analyze the impact of capacitance on the laser's electrical parameters, the laser is divided into areas separated by appropriately chosen equipotential surfaces. Then, an equivalent circuit is built as shown in figure 12. The capac-

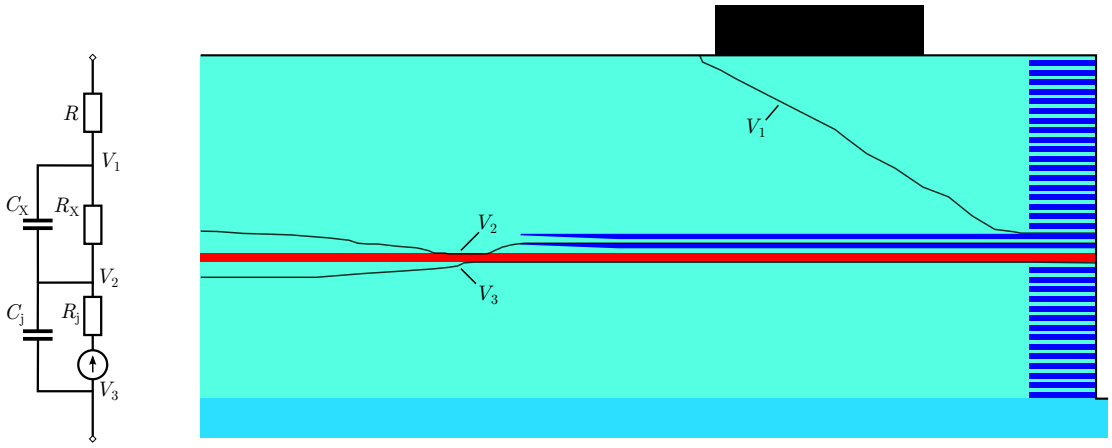

Figure 12. Partition of a VCSEL by equivalent surfaces and the resulting equivalent circuit [92]. For the laser structure a cylindrical symmetry as in figure 11 is assumed.

itances are determined in the way described above, while the resistances are determined based on the simulated current ad potential differences between the equipotential surfaces.

We have verified the validity of our model by comparing the calculated values of the complex impedance of lasers with impedances measured in small signal modulation reflection (SSMR) experiment, for modulation frequencies up to 40 GHz. The results are pre-

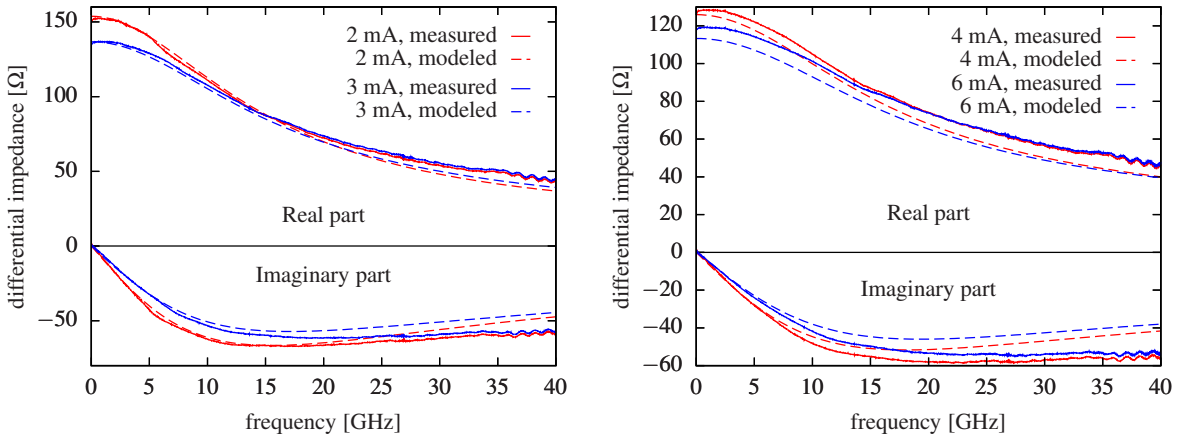

Figure 13. Results obtained using the capacitance.model. Comparison of predicted by the model (dashed lines) and measured (solid lines) complex impedances of a VCSEL as functions of modulation frequency [9]. The calculations and measurements were performed for two above-threshold currents.

sented in figure 13. Very good agreement between the theoretical and experimental results can be seen for frequencies up to around 20 GHz. The fact that the calculated modulus of

the impedance is too low at higher frequencies can be at least partially explained by the expected decrease in the permittivity. Due to the lack of appropriate material data, we assumed a constant value equal to the static value of the permittivity.

The laser's impedance is not the only information which can be obtained using the model. For the equivalent circuit it is possible to solve a set of differential equations for the currents flowing through its elements. This is a method for finding the distortions of the current signal. Solutions $I_l(t)$ of the set of differential equations are linear combinations of decaying exponential functions and a function $I_l^{\infty}(t)$ determined by the shape of the voltage signal.

$$I_l(t) = I_l^{\infty}(t) + A_l^{(1)} \exp(\lambda_1 t) + \cdots + A_l^{(n)} \exp(\lambda_n t) \tag{24}$$

Parameters λ_i are negative eigenvalues of the matrix describing this set of differential equations. The dimension of this matrix depend on the number of the elements in the equivalent circuit. Constants A_l are determined based on the initial conditions.

Capacitance is not the only factor that limits the modulation frequency in semiconductor lasers. The dynamics of the photons in the cavity and carrier recombination processes in the active region also play very important roles. These processes are described by the following rate equations for the number of photons and carriers [93]:

$$\frac{dN}{dt} = F_1(N,P) + \frac{1}{e} I(t) \tag{25}$$

$$\frac{dP}{dt} = F_2(N,P) \tag{26}$$

where N, P are the numbers of carriers and photons respectively, F_1 and F_2 are functions describing carrier recombination and photon generation (or absorption), I is the current flowing through the laser and e is the elementary charge. Functions F_1 and F_2 can, in the case of small signal modulation, be approximated by the following linear functions:

$$F_1(N,P) = \gamma_{11} N(t) + \gamma_{12} P(t) \tag{27}$$

$$F_2(N,P) = \gamma_{21} N(t) + \gamma_{22} P(t) \tag{28}$$

Solving of system (25) in the linear approximation is a standard procedure. For currents described by linear combinations of exponents and trigonometric functions (as is usually the case for the modulation voltages used in modulation experiments) the solution can be given in an analytic form. The problem lies in finding appropriate values for the equation's parameters. So far, in the literature, the solutions of (25) have been fitted to experimental data which is not satisfactory. Thank to our model it should be possible to calculate these parameters based on the structure's design. For instance, parameter γ_{22} is the photon life time in the cavity, which can be computed using an optical model. The other parameters can be found using the idea and calculations that my model of above-threshold laser operation is based on, presented in [2]. I have already started working on this model. which would be the first model capable of predicting the modulation parameters of semiconductor lasers.

8. Summary

The papers presented here concern theoretical calculations (numerical analysis, quantum-mechanical calculations) and modelling of various types of semiconductor laser:

edge and surface emitting, electrically and optically pumped, with active regions containing quantum wells, quantum dots and superlattices. Most of the work was carried out in co-operation with technology laboratories and was used in the fabrication of real devices. Each type of active region required a separate model of the optical gain. The most challenging aspect (especially in terms of numerical implementation) was the modelling of superlattices, despite the fact it was not a full gain model. On the other hand, creation of the capacitance model required a very different approach to laser modelling.

One of the main obstacles to the modelling of modern devices is the lack of consistent data on the values of material parameters. Usually, such devices contain materials or structures which have not been analyzed closely. Close co-operation with experimentalists and access to the results of many measurements (and not only to those that are most satisfactory, those being most usually published) is then invaluable. It is worth remembering that experimental results in the form of numbers and graphs, even if presented in the best possible way, do not reveal all the information obtained during the measurements. This lost information may concern matters which are difficult to express in numbers or which the experimentalist considers (possibly erroneously) unimportant or obvious. For these reasons, performing or assisting in experiments oneself is extremely important.

Even in ideal situations, however, one should not expect the modelling of such complicated systems using under-researched materials to provide quantitatively exact results. Devices in the early stages of their development may have very different parameters, despite the fact that they are in other respects nominally identical. This is not, of course, the only cause of discrepancies between calculations and measurements. In the Preface, it was mentioned that the simplification of models allows for applications to more complex situations. However, further simplification is often needed. The fact that we can write equations on a piece of paper does not mean that finding their solutions will be swift or straightforward (and such solutions are usually only numerical, since analytic solutions are a rare luxury). Despite the fact we live in only three dimensions, even in the case of the most fundamental equations, such as Maxwell's equations or transport equations (of heat, current), finding solutions (especially if they are self-consistent) is still extremely time consuming. For this reason, any symmetry in a problem, which allows its dimensions to be reduced, is very welcome. Often, the modelled structure is somewhat simplified in order to attain such symmetry. Fortunately, the error induced by such simplification can often be estimated by performing a single calculation for both the simplified and non-simplified cases. If this test shows that the difference is small enough, the remaining calculations can be performed using the simplified model.

Solid state quantum modelling is more difficult. It is not possible to perform non-simplified calculations, so the main criterion of the validity of the model is its consistency with experiment. Moreover, it is usually difficult to measure values which are directly related to such calculations. For these reasons, different kinds of model are used. Even so, the case of quantum cascade lasers has shown that even a very simplified model (an envelope function approximation) can be successfully used to find electronic states even at higher energy levels.

Despite the fact that a model is not always able to predict the exact experimental characteristics of a device, modelling can be a very efficient way to predict whether a modification that is being considered will produce favorable results (or if its implementation is worth

the effort). The other important use is in predicting the theoretical limits of the device's parameters, since modelling usually idealises the situation. This, however, need not be always true. The model takes into account only those phenomena which have been included in its construction. This is a very important factor, which occasionally causes the use of (especially commercial) computer models to be misleading, due to the lack of information on how they work.

Of course, there are also situations when creating a device is impossible without advanced modelling. Quantum cascade lasers are again a very good example, in which the structure of electronic states must fulfill several subtle conditions. In any case, creating a realistic model can save a lot of money and time when developing devices, and allows a deeper understanding of what is occurring within them.

In this review I presented only a part, though very important, of my scientific activity. The following achievements I personally consider most valuable.

1. Devising the capacitance model and the basis for a model of modulation properties of semiconductor lasers and their application to analysis of VCSELs. Despite the fact that this model was created only recently, it allowed to predict that VCSEL structures can be significantly simplified without worsening their modulation properties. Experimental results, unpublished yet, confirm these conclusions.
2. Devising the above-threshold model for semiconductor lasers. It differs from the models that can be found in the literature, and, like the capacitance model, is adjusted to the models developed by or group, being their expansion. The work on this model allowed for optimization of threshold calculations, thanks to the analysis of convergence of the algorithms used, I performed.
3. Implementation of an optical gain model which has been included in the simulation software developed by our group. Results obtained using this model were used in a great number of publications of our group.

From the things not described in this review:

4. Initiation of experimental investigations concerning characterization of devices and determination of material parameters used in semiconductor lasers. As a result, one paper [94] has already been published, and measurements performed in our group's laboratory (under development) have already given valuable, from the point of view of laser's modelling, data. Such data are usually not available in the literature. Moreover, the success (so far) of these investigations confirms my conviction that the categorisation of physicists as either experimentalists or theoreticians is in general wrong.

Besides, the fact that all the students whose MSc supervisor I was, continue scientific career in various institutions. Most of them have already got their PhD.

References

[11] Andrzej K. Wróblewski. "Prawda i mity w fizyce". In: Iskry, 1987. Chap. Nauka na manowcach.

[12] Richard P. Feynman. "QED. Osobliwa teoria światła i materii". In: Prószyński i S-ka,

[13] R.N. Hall, G.E. Fenner, J.D. Kingsley, T.J. Soltys, and R.O. Carlson. "Coherent Light Emission From GaAs Junctions". In: *Phys. Rev. Lett.* 9 (9 Nov. 1962), pp. 366–368. DOI: 10.1103/PhysRevLett.9.366. URL: http://link.aps.org/doi/10.1103/PhysRevLett.9.366.

[14] Marshall I. Nathan, William P. Dumke, Gerald Burns, Jr. Frederick H. Dill, and Gordon Lasher. "Stimulated emission of radiation from GaAs p-n junctions". In: *Applied Physics Letters* 1.3 (1962), pp. 62–64. DOI: 10.1063/1.1777371. URL: http://link.aip.org/link/?APL/1/62/1.

[15] Nick Holonyak Jr. and S.F. Bevacqua. "Coherent (visible) light emission from $Ga(As_{1-x}P_x)$ junctions". In: *Applied Physics Letters* 1.4 (1962), pp. 82–83. DOI: 10.1063/1.1753706. URL: http://link.aip.org/link/?APL/1/82/1.

[16] I. Hayashi, M. B. Panish, P. W. Foy, and S. Sumski. "Junction lasers which operate continuously at room temperature". In: *Applied Physics Letters* 17.3 (1970), pp. 109–111. DOI: 10.1063/1.1653326. URL: http://link.aip.org/link/?APL/17/109/1.

[17] R.D. Dupuis, P.D. Dapkus, N. Holonyak, E.A. Rezek, and A. Chin. "Room-temperature laser operation of quantum-well Ga(1-x)AlxAs-GaAs laser diodes grown by metalorganic chemical vapor deposition". In: *Applied Physics Letters* 32.5 (1978), pp. 295–297. ISSN: 0003-6951. DOI: 10.1063/1.90026.

[18] D. Xu, C. Tong, S.F. Yoon, W. Fan, D.H. Zhang, M. Wasiak, Ł. Piskorski, K. Gutowski, R.P. Sarzała, and W. Nakwaski. "Room-temperature continuous-wave operation of the In(Ga)As/GaAs quantum-dot VCSELs for the 1.3 μm optical-fibre communication". In: *Semicond. Sci. Technol.* 24 (2009).

[19] Jerome Faist, Federico Capasso, Deborah L. Sivco, Carlo Sirtori, Albert L. Hutchinson, and Alfred Y. Cho. "Quantum Cascade Laser". In: *Science* 264.5158 (1994), pp. 553–556. DOI: 10.1126/science.264.5158.553.

[20] Jerome Faist, Federico Capasso, Deborah L. Sivco, Albert L. Hutchinson, Carlo Sirtori, S. N. G. Chu, and Alfred Y. Cho. "Quantum cascade laser: Temperature dependence of the performance characteristics and high T_0 operation". In: *Applied Physics Letters* 65.23 (1994), pp. 2901–2903. DOI: 10.1063/1.112524. URL: http://link.aip.org/link/?APL/65/2901/1.

[21] J. Faist, F. Capasso, D.L. Sivco, C. Sirtori, A.L. Hutchinson, and A.Y. Cho. "Quantum cascade laser: an intersub-band semiconductor laser operating above liquid nitrogen temperature". In: *Electronics Letters* 30.11 (May 1994), pp. 865–866. ISSN: 0013-5194. DOI: 10.1049/el:19940605.

[22] F. Capasso, J. Faist, D.L. Sivco, C. Sirtori, A.L. Hutchinson, S.N.G. Chu, and A.Y. Cho. "Quantum cascade laser: a unipolar intersubband semiconductor laser". In: *Semiconductor Laser Conference, 1994., 14th IEEE International*. Sept. 1994, pp. 71–72. DOI: 10.1109/ISLC.1994.519139.

[23] Benjamin S. Williams. "GaAs/AlGaAs mid-infrared quantum cascade laser". MA thesis. Massachusetts Institute of Technology, Dept. of Electrical Engineering and Computer Science, 1998.

[24] G. Strasser, S. Gianordoli, L. Hvozdara, W. Schrenk, K. Unterrainer, and E. Gornik. "GaAs/AlGaAs superlattice quantum cascade lasers at $\lambda \approx 13\,\mu m$". In: *Applied Physics Letters* 75.10 (1999), pp. 1345–1347. DOI: 10.1063/1.124688. URL: http://link.aip.org/link/?APL/75/1345/1.

[25] H. Page, P. Kruck, S. Barbieri, C. Sirtori, M. Stellmacher, and J. Nagle. "High peak power (1.1 W) (Al)GaAs quantum cascade laser emitting at 9.7 µm". In: *Electronics Letters* 35.21 (Oct. 1999), pp. 1848–1849. ISSN: 0013-5194. DOI: 10.1049/el:19991268.

[26] Kamil Kosiel, Maciej Bugajski, Anna Szerling, Justyna Kubacka-Traczyk, Piotr Karbownik, Emilia Pruszyńska-Karbownik, Jan Muszalski, Adam Łaszcz, Przemek Romanowski, Michał Wasiak, Włodzimierz Nakwaski, Irina Makarowa, and Piotr Perlin. "77 K operation of AlGaAs/GaAs quantum cascade laser at 9 µm". In: *Photonics Letters of Poland* 1 (2009), pp. 16–18.

[27] Y. Arakawa and H. Sakaki. "Multidimensional quantum well laser and temperature dependence of its threshold current". In: *Applied Physics Letters* 40.11 (1982), pp. 939–941. DOI: 10.1063/1.92959. URL: http://link.aip.org/link/?APL/40/939/1.

[28] А.И. Екимов and А.А. Онущенко. "Квантовый размерный эффект в трехмерных микрокристаллах полупроводников". In: *Письма в ЖЭТФ.* 34 (1981), pp. 363–366.

[29] A.I. Ekimov and A.A. Onushchenko. "Quantum size effect in three-dimensional microscopic semiconductor crystals". In: *Journal of Experimental and Theoretical Physics Letters* 34 (1981), pp. 345–348.

[30] N. Kirstaedter, N.N. Ledentsov, M. Grundmann, D. Bimberg, V.M. Ustinov, S.S. Ruvimov, M.V. Maximov, P.S. Kop'ev, Zh.I. Alferov, U. Richter, P. Werner, U. Gosele, and J. Heydenreich. "Low threshold, large T_0 injection laser emission from (InGa)As quantum dots". In: *Electronics Letters* 30.17 (1994), pp. 1416–1417. ISSN: 0013-5194. DOI: 10.1049/el:19940939.

[31] H. Shoji, K. Mukai, N. Ohtsuka, M. Sugawara, T. Uchida, and H. Ishikawa. "Lasing at three-dimensionally quantum-confined sublevel of self-organized $In_{0.5}Ga_{0.5}As$ quantum dots by current injection". In: *Photonics Technology Letters, IEEE* 7.12 (1995), pp. 1385–1387. ISSN: 1041-1135. DOI: 10.1109/68.477257.

[32] K. Mukai, Y. Nakata, Koji Otsubo, M. Sugawara, Naoki Yokoyama, and H. Ishikawa. "1.3-µm CW lasing of InGaAs-GaAs quantum dots at room temperature with a threshold current of 8 mA". In: *Photonics Technology Letters, IEEE* 11.10 (1999), pp. 1205–1207. ISSN: 1041-1135. DOI: 10.1109/68.789692.

[33] G. Park, O.B. Shchekin, D.L. Huffaker, and D.G. Deppe. "Low-threshold oxide-confined 1.3-µm quantum-dot laser". In: *Photonics Technology Letters, IEEE* 12.3 (2000), pp. 230–232. ISSN: 1041-1135. DOI: 10.1109/68.826897.

[34] I.R. Sellers, H-Y Liu, K.M. Groom, D.T. Childs, D. Robbins, T.J. Badcock, M. Hopkinson, D.J. Mowbray, and M.S. Skolnick. "1.3 µm InAs/GaAs multilayer quantum-dot laser with extremely low room-temperature threshold current density". In: *Electronics Letters* 40.22 (2004), pp. 1412–1413. ISSN: 0013-5194. DOI: 10.1049/el:20046692.

[35] D.G. Deppe, S. Freisem, G. Ozgur, K. Shavritranuruk, and H. Chen. "Very low threshold current density continuous-wave quantum dot laser diode". In: *Semiconductor Laser Conference, 2008. ISLC 2008. IEEE 21st International*. 2008, pp. 33–34. DOI: 10.1109/ISLC.2008.4635995.

[36] E. C. Le Ru, P. Howe, T. S. Jones, and R. Murray. "Strain-engineered InAs/GaAs quantum dots for long-wavelength emission". In: *Phys. Rev. B* 67 (16 Apr. 2003), p. 165303. DOI: 10.1103/PhysRevB.67.165303. URL: http://link.aps.org/doi/10.1103/PhysRevB.67.165303.

[37] M.A. Majid, D. T D Childs, H. Shahid, Siming Chen, K. Kennedy, R.J. Airey, R.A. Hogg, Edmund Clarke, P. Howe, P.D. Spencer, and Ray Murray. "Toward 1550-nm GaAs-Based Lasers Using InAs/GaAs Quantum Dot Bilayers". In: *Selected Topics in Quantum Electronics, IEEE Journal of* 17.5 (2011), pp. 1334–1342. ISSN: 1077-260X. DOI: 10.1109/JSTQE.2011.2108270.

[38] E. Clarke, P. Spencer, E. Harbord, P. Howe, and R. Murray. "Growth, optical properties and device characterisation of InAs/GaAs quantum dot bilayers". In: *Journal of Physics: Conference Series* 107.1 (2008), p. 012003. URL: http://stacks.iop.org/1742-6596/107/i=1/a=012003.

[39] Y. Ben-Ezra M. Haridim B.I. Lembrikov. "Advances in Optical Amplifiers". In: InTech, 2011. Chap. Semiconductor Optical Amplifiers.

[40] Z.Y. Zhang, A.E.H. Oehler, B. Resan, S. Kurmulis, K.J. Zhou, Q. Wang, M. Mangold, T. Süedmeyer, U. Keller, K.J. Weingarten, and R.A. Hogg. "1.55 µm InAs/GaAs Quantum Dots and High Repetition Rate Quantum Dot SESAM Mode-locked Laser". In: *Sci. Rep.* 2 (2012).

[41] A. Mohan, M. Felici, P. Gallo, B. Dwir, A. Rudra, J. Faist, and E. Kapon. "Polarization-entangled photons produced with high-symmetry site-controlled quantum dots". In: *Nature Photonics* 4 (2010), pp. 302–306.

[42] Gediminas Juska, Valeria Dimastrodonato, Lorenzo O. Mereni, and Agnieszka Gocalinska and Emanuele Pelucchi. "Towards quantum-dot arrays of entangled photon emitters". In: *Nature Photonics* 7 (2013), pp. 527–531.

[43] Wlodzimierz Nakwaski, Robert P. Sarzala, M. Wasiak, T. Czyszanowski, and Pawel Mackowiak. *Single-photon devices in quantum cryptography*. 2003. DOI: 10.1117/12.519752. URL: http://dx.doi.org/10.1117/12.519752.

[44] Julien Claudon, Joël Bleuse, Nitin Singh Malik, Maela Bazin, Périne Jaffrennou, Niels Gregersen, Christophe Sauvan, Philippe Lalanne, and Jean-Michel Gérard. "A highly efficient single-photon source based on a quantum dot in a photonic nanowire". In: *Nature Photonics* 4 (2010), pp. 174–177.

[45] Kohki Mukai, Nobuyuki Ohtsuka, Hajime Shoji, and Mitsuru Sugawara. "Growth and optical evaluation of InGaAs/GaAs quantum dots self-formed during alternate supply of precursors". In: *Applied Surface Science* 112.0 (1997), pp. 102–109. ISSN: 0169-4332. DOI: http://dx.doi.org/10.1016/S0169-4332(96)00993-2. URL: http://www.sciencedirect.com/science/article/pii/S0169433296009932.

[46] S.H. Pyun and W.G. Jeong. "Luminescence Characteristics of InGaAs/GaAs Quantum Dots Emitting Near 1.5 µm". In: *Journal of the Korean Physical Society* 56 (2010), pp. 586–590.

[47] Arkadiusz Wojs, Pawel Hawrylak, Simon Fafard, and Lucjan Jacak. "Electronic structure and magneto-optics of self-assembled quantum dots". In: *Phys. Rev. B* 54 (8 Aug. 1996), pp. 5604–5608. DOI: 10.1103/PhysRevB.54.5604. URL: http://link.aps.org/doi/10.1103/PhysRevB.54.5604.

[48] Stephanie M. Reimann and Matti Manninen. "Electronic structure of quantum dots". In: *Rev. Mod. Phys.* 74 (4 Nov. 2002), pp. 1283–1342. DOI: 10.1103/RevModPhys.74.1283. URL: http://link.aps.org/doi/10.1103/RevModPhys.74.1283.

[49] A. Markus, J.X. Chen, C. Paranthoen, A. Fiore, C. Platz, and O. Gauthier-Lafaye. "Simultaneous two-state lasing in quantum-dot lasers". In: *Applied Physics Letters* 82.12 (2003), pp. 1818–1820. ISSN: 0003-6951. DOI: 10.1063/1.1563742.

[50] Hsing-Yeh Wang, Hsu-Chieh Cheng, Sheng-Di Lin, and Chien-Ping Lee. "Wavelength switching transition in quantum dot lasers". In: *Applied Physics Letters* 90.8, 081112 (2007). DOI: http://dx.doi.org/10.1063/1.2709987. URL: http://scitation.aip.org/content/aip/journal/apl/90/8/10.1063/1.2709987.

[51] Y. Ding, W.J. Fan, B.S. Ma, D.W. Xu, S.F. Yoon, S. Liang, L.J. Zhao, M. Wasiak, T. Czyszanowski, and W. Nakwaski. "Microphotoluminescence investigation of InAs quantum dot active region in 1.3 μm vertical cavity surface emitting laser structure". In: *Journal of Applied Physics* 108.7 (2010). ISSN: 0021-8979. DOI: 10.1063/1.3490236.

[52] Tsuei-Lian Wang, Y. Kaneda, J.M. Yarborough, J. Hader, J.V. Moloney, A. Chernikov, S. Chatterjee, S.W. Koch, B. Kunert, and W. Stolz. "High-Power Optically Pumped Semiconductor Laser at 1040 nm". In: *Photonics Technology Letters, IEEE* 22.9 (May 2010), pp. 661–663. ISSN: 1041-1135. DOI: 10.1109/LPT.2010.2043731.

[53] W. B. Jiang, S. R. Friberg, H. Iwamura, and Y. Yamamoto. "High powers and subpicosecond pulses from an external-cavity surface-emitting InGaAs/InP multiple quantum well laser". In: *Applied Physics Letters* 58.8 (Feb. 1991), pp. 807–809. ISSN: 0003-6951. DOI: 10.1063/1.104495.

[54] B. Heinen, T.-L. Wang, M. Sparenberg, A. Weber, B. Kunert, J. Hader, S.W. Koch, J.V. Moloney, M. Koch, and W. Stolz. "106 W continuous-wave output power from vertical-external-cavity surface-emitting laser". In: *Electronics Letters* 48.9 (2012), pp. 516–517. ISSN: 0013-5194. DOI: 10.1049/el.2012.0531.

[55] Jill D. Berger, Douglas W. Anthon, Andrea Caprara, Juan L. Chilla, Sergei V. Govorkov, Arnaud Y. Lepert, Wayne Mefferd, Qi-Ze Shu, and Luis Spinelli. "20 Watt CW TEM_{00} intracavity doubled optically pumped semiconductor laser at 532 nm". In: (2012). DOI: 10.1117/12.907511. URL: +%20http://dx.doi.org/10.1117/12.907511.

[56] A. Rantamäki, A. Sirbu, A. Mereuta, E. Kapon, and O. G. Okhotnikov. "3 W of 650 nm red emission by frequency doubling of wafer-fused semiconductor disk laser". In: *Optics Express* 18.21 (2010), pp. 21645–21650.

[57] M. Guina, A. Härkönen, V.M. Korpijärvi, T. Leinonen, and S. Suomalainen. "Semiconductor Disk Lasers: Recent Advances in Generation of Yellow-Orange and Mid-IR Radiation". In: *Advances in Optical Technologies* (2012).

[58] A. Sirbu, N. Volet, A. Mereuta, J. Lyytikäinen, J. Rautiainen, O. Okhotnikov, J. Walczak, M. Wasiak, T. Czyszanowski, A. Caliman, Q. Zhu, V. Iakovlev, and E. Kapon.

"Wafer-Fused Optically Pumped VECSELs Emitting in the 1310-nm and 1550-nm Wavebands". In: *Advances in Optical Technologies* (2011).

[59] A. Jasik, A.K. Sokół, A. Broda, I. Sankowska, A. Wójcik-Jedlińska, A. Trajnerowicz, M. Wasiak, J. Kubacka-Traczyk, and J. Muszalski. "Strain impact on periodic gain structures on Vertical External Cavity Surface-Emitting Lasers". in preparation.

[60] A. Jasik, A. Sokół, J. Muszalski, A.Wójcik-Jedlińska, J. Kubacka-Traczyk, A. Broda, M. Wasiak, I. Sankowska, and A. Trajnerowicz. "Dual-wavelength vertical external cavity surface emitting laser – simplified design and strict growth control". in preparation.

[61] J. Muszalski, A. Broda, A. Trajnerowicz, A. Wójcik-Jedlińska, R.P. Sarzała, M. Wasiak, P. Gutowski, I. Sankowska, J. Kubacka-Traczyk, and K. Gołaszewska-Malec. "Switchable double wavelength generating vertical external cavity surface-emitting laser". In: *Opt. Express* 22 (2014), pp. 6447–6452.

[62] K.S. Kim, J.R. Yoo, S.H. Cho, S.M. Lee, S.J. Lim, J.Y. Kim, J.H. Lee, T. Kim, and Y.J. Park. "1060 nm vertical-external-cavity surface-emitting lasers with an optical-to-optical efficiency of 44% at room temperature". In: *Applied Physics Letters* 88.9, 091107 (2006), p. 091107. DOI: 10.1063/1.2181272. URL: http://link.aip.org/link/?APL/88/091107/1.

[63] Li Fan, J. Hader, Marc Schillgalies, M. Fallahi, Aramais R. Zakharian, J.V. Moloney, Robert Bedford, James T. Murray, S.W. Koch, and W. Stolz. "High-power optically pumped VECSEL using a double-well resonant periodic gain structure". In: *Photonics Technology Letters, IEEE* 17.9 (2005), pp. 1764–1766. ISSN: 1041-1135. DOI: 10.1109/LPT.2005.853536.

[64] M. Gębski, O. Kuzior, M. Dems, M. Wasiak, Y.Y. Xie, Z.J. Xu, Q.J. Wang, D.H. Zhang, and T. Czyszanowski. "Transverse mode control in high-contrast grating VCSELs". In: *Optics Express* 22.17 (2014), pp. 20954–20963.

[65] Marcin Gębski, Maciej Dems, Michał Wasiak, Robert P. Sarzała, J.A. Lott, and Tomasz Czyszanowski. "Double high refractive-index contrast grating VCSEL". In: *Proc. SPIE* 9381 (2015), 93810Q-93810Q-7. DOI: 10.1117/12.2079328. URL: http://dx.doi.org/10.1117/12.2079328.

[66] M. Gebski, O. Kuzior, M. Wasiak, A. Szerling, A. Wójcik-Jedlińska, N. Pałka, M. Dems, Y. Y. Xie, Z. J. Xu, Q. J. Wang, D. H. Zhang, and T. Czyszanowski. "High-contrast grating reflectors for 980 nm vertical-cavity surface-emitting lasers". In: *Proc. SPIE* 9372 (2015), pp. 937206-937206-9. DOI: 10.1117/12.2080989. URL: http://dx.doi.org/10.1117/12.2080989.

[67] M. Gębski, M. Dems, A. Szerling, M. Motyka, L. Marona, R. Kruszka, D. Urbańczyk, M. Walczakowski, N. Pałka, A. Wójcik-Jedlińska, Q. J. Wang, D. H. Zhang, M. Bugajski, M. Wasiak, and T. Czyszanowski. "Monolithic high-index contrast grating: a material independent high-reflectance VCSEL mirror". In: *Opt. Express* 23.9 (May 2015), pp. 11674–11686. DOI: 10.1364/OE.23.011674.

[68] M. Gębski, M. Dems, M. Wasiak, J. A. Lott, and T. Czyszanowski. "Monolithic Subwavelength High-Index-Contrast Grating VCSEL". In: *IEEE Photonics Technology Letters* 27.18 (Sept. 2015), pp. 1953–1956. ISSN: 1041-1135. DOI: 10.1109/LPT.2015.2447932.

[69] Czyszanowski Tomasz, Gębski Marcin, Dems Maciej, Wasiak Michał, Sarzała Robert, and Panajotov Krassimir. "Subwavelength grating as both emission mirror and electrical contact for VCSELs in any material system". In: *Scientific Reports* 7 (Jan. 2017), p. 40348. DOI: http://dx.doi.org/10.1038/srep4034810.1038/srep40348.

[70] C. Schow, F. Doany, and J. Kash. "Get on the optical bus". In: *Spectrum, IEEE* 47.9 (Sept. 2010), pp. 32–56. ISSN: 0018-9235. DOI: 10.1109/MSPEC.2010.5557513.

[71] Kai Chen, A. Singla, A. Singh, K. Ramachandran, Lei Xu, Yueping Zhang, Xitao Wen, and Yan Chen. "OSA: An optical switching architecture for data center networks with unprecedented flexibility". In: *Networking, IEEE/ACM Transactions on* 22.2 (Apr. 2014), pp. 498–511. ISSN: 1063-6692. DOI: 10.1109/TNET.2013.2253120.

[72] F.E. Doany, C.L. Schow, B.G. Lee, R.A. Budd, C.W. Baks, C.K. Tsang, J.U. Knickerbocker, R. Dangel, B. Chan, How Lin, C. Carver, Jianzhuang Huang, J. Berry, D. Bajkowski, F. Libsch, and J.A. Kash. "Terabit/s-class optical PCB links incorporating 360-Gb/s bidirectional 850 nm parallel optical transceivers". In: *Lightwave Technology, Journal of* 30.4 (Feb. 2012), pp. 560–571. ISSN: 0733-8724. DOI: 10.1109/JLT.2011.2177244.

[73] F. Doany. *Power-efficient, high-bandwidth optical interconnects for high performance computing*. Hot Interconnects. Aug. 2012.

[74] P. Moser, J.A. Lott, and D. Bimberg. "Energy Efficiency of Directly Modulated Oxide-Confined High Bit Rate 850-nm VCSELs for Optical Interconnects". In: *Selected Topics in Quantum Electronics, IEEE Journal of* 19.4 (July 2013), p. 1702212. ISSN: 1077-260X. DOI: 10.1109/JSTQE.2013.2255266.

[75] P. Westbergh, R. Safaisini, Å Haglund, B. Kögel, J.S. Gustavsson, A. Larsson, M. Geen, R. Lawrence, and A. Joel. "High-speed 850 nm VCSELs with 28 GHz modulation bandwidth operating error-free up to 44 Gbit/s". In: *Electronics Letters* 48 (18 Aug. 2012), 1145–1147(2). ISSN: 0013-5194. URL: http://digital-library.theiet.org/content/journals/10.1049/el.2012.2525.

[76] Chih-Hao Chang, L. Chrostowski, and C.J. Chang-Hasnain. "Parasitics and design considerations on oxide-implant VCSELs". In: *Photonics Technology Letters, IEEE* 13.12 (Dec. 2001), pp. 1274–1276. ISSN: 1041-1135. DOI: 10.1109/68.969879.

[77] H. Li, P. Wolf, P. Moser, G. Larisch, J.A. Lott, and D. Bimberg. "Temperature-Stable 980-nm VCSELs for 35-Gb/s Operation at 85°C With 139-fJ/bit Dissipated Heat". In: *Photonics Technology Letters, IEEE* 26.23 (Dec. 2014), pp. 2349–2352. ISSN: 1041-1135. DOI: 10.1109/LPT.2014.2354736.

[78] P. Moser, J.A. Lott, G. Larisch, and D. Bimberg. "Impact of the Oxide-Aperture Diameter on the Energy-Efficiency, Bandwidth, and Temperature Stability of 980-nm VCSELs". In: *J. Lightwave Technol.* 33.4 (Feb. 2015), pp. 825–831. DOI: 10.1109/JLT.2014.2365237.

[79] P. Westbergh, J.S. Gustavsson, B. Kögel, Å. Haglund, and A. Larsson. "Impact of Photon Lifetime on High-Speed VCSEL Performance". In: *Selected Topics in Quantum Electronics, IEEE Journal of* 17.6 (Nov. 2011), pp. 1603–1613. ISSN: 1077-260X. DOI: 10.1109/JSTQE.2011.2114642.

[80] H. Li, J.A. Lott, P. Wolf, P. Moser, G. Larisch, and D. Bimberg. "Temperature-Dependent Impedance Characteristics of Temperature-Stable

High-Speed 980-nm VCSELs". In: *Photonics Technology Letters, IEEE* 27.8 (Apr. 2015), pp. 832–835. ISSN: 1041-1135. DOI: 10.1109/LPT.2015.2393863.

[81] P. Westbergh, J.S. Gustavsson, A. Haglund, M. Skold, A. Joel, and A. Larsson. "High-Speed, Low-Current-Density 850 nm VCSELs". In: *Selected Topics in Quantum Electronics, IEEE Journal of* 15.3 (May 2009), pp. 694–703. ISSN: 1077-260X. DOI: 10.1109/JSTQE.2009.2015465.

[82] K.L. Lear, V.M. Hietala, H.Q. Hou, M. Ochiai, J.J. Banas, B.E. Hammons, J.C. Zolper, and S.P. Kilcoyne. "Small and large signal modulation of 850 nm oxide-confined vertical cavity surface emitting lasers". In: *Advances in Vertical Cavity Surface Emitting Lasers in Trends in Optics and Photonics Series* 15 (1997), pp. 69–74.

[83] Y. Liu, W.-C. Ng, F. Oyafuso, B. Klein, and K. Hess. "Simulating the modulation response of VCSELs: the effects of diffusion capacitance and spatial hole-burning". In: *IEE Proceedings–Optoelectronics*. Vol. 149. 4. IET. 2002, pp. 182–188.

[84] J. Strologas and K. Hess. "Diffusion capacitance and laser diodes". In: *Electron Devices, IEEE Transactions on* 51.3 (Mar. 2004), pp. 506–509. ISSN: 0018-9383. DOI: 10.1109/TED.2003.822345.

[85] L.F. Feng, C.D. Wang, H.X. Cong, C.Y. Zhu, Jun Wang, X.S. Xie, C.Z. Lu, and G.Y. Zhang. "Sudden change of electrical characteristics at lasing threshold of a semiconductor laser". In: *Quantum Electronics, IEEE Journal of* 43.6 (June 2007), pp. 458–461. ISSN: 0018-9197. DOI: 10.1109/JQE.2007.895663.

[86] A.N. Al-Omari and K.L. Lear. "Polyimide-planarized vertical-cavity surface-emitting lasers with 17.0-GHz bandwidth". In: *Photonics Technology Letters, IEEE* 16.4 (Apr. 2004), pp. 969–971. ISSN: 1041-1135. DOI: 10.1109/LPT.2004.824622.

[87] Y. Ou, J.S. Gustavsson, P. Westbergh, Å. Haglund, A. Larsson, and A. Joel. "Impedance Characteristics and Parasitic Speed Limitations of High-Speed 850-nm VCSELs". In: *Photonics Technology Letters, IEEE* 21.24 (Dec. 2009), pp. 1840–1842. ISSN: 1041-1135. DOI: 10.1109/LPT.2009.2034618.

[88] M. Grabherr, S. Intemann, S. Wabra, P. Gerlach, M. Riedl, and R. King. "25 Gbps and beyond: VCSEL development at Philips". In: *Proc. SPIE* 8639 (2013).

[89] P. Westbergh. "High Speed Vertical Cavity Surface Emitting Lasers for Short Reach Communication". PhD thesis. Chalmers University of Technology, 2011. ISBN: 978-91-7385-527-3.

[90] Yu-Chia Chang and L.A. Coldren. "Efficient, High-Data-Rate, Tapered Oxide-Aperture Vertical-Cavity Surface-Emitting Lasers". In: *Selected Topics in Quantum Electronics, IEEE Journal of* 15.3 (May 2009), pp. 704–715. ISSN: 1077-260X. DOI: 10.1109/JSTQE.2008.2010955.

[91] "Basic Small Signal Modulation Response". English. In: *Ultra-high Frequency Linear Fiber Optic Systems*. Ed. by Kam Y. Lau. Springer Berlin Heidelberg, 2009, pp. 11–18. ISBN: 978-3-540-25350-1. DOI: 10.1007/978-3-540-49906-0_2. URL: http://dx.doi.org/10.1007/978-3-540-49906-0_2.

[92] Michał Wasiak, Patrycja Śpiewak, Philip Moser, and James A. Lott. *Capacitance and modulation time constant in oxide-confined vertical-cavity surface-emitting lasers with different oxide layers*. 2016. DOI: 10.1117/12.2230312. URL: http://dx.doi.org/10.1117/12.2230312.

[93] LA Coldren and SW Corzine. *Diode lasers and photonic integrated circuits*. John Wiley & Sons, 1995.

[94] Michał Wasiak, Jarosław Walczak, Marcin Motyka, Filip Janiak, Artur Trajnerowicz, and Agata Jasik. "Below-band-gap absorption in undoped GaAs at elevated temperatures". In: *Optical Materials* 64 (2017), pp. 137–141. ISSN: 0925-3467. DOI: https://doi.org/10.1016/j.optmat.2016.11.028.